RESEARCH ARTICLE

WILEY

Statistical QoS guarantees of a device-to-device link assisted by a full-duplex relay

Syed Waqas Haider Shah[1,2] | Rongpeng Li[1,3] |
Muhammad Mahboob Ur Rahman[4] | Adnan Noor Mian[4] |
Waqas Aman[4] | Jon Crowcroft[1]

[1]Computer Laboratory, University of Cambridge, Cambridge, UK

[2]Department of Electrical Engineering, Information Technology University, Lahore, Pakistan

[3]Zhejiang University, Hangzhou, China

[4]Computer Science Department, Information Technology University, Lahore, Pakistan

Correspondence to:
Syed Waqas Haider Shah, Computer Laboratory, University of Cambridge, 15 JJ Thomson Avenue, Cambridge CB3 0FD, UK.
Email:sw920@cl.cam.ac.uk
waqas.haider@itu.edu.pk

Abstract

Device-to-device (D2D) communication is a promising technique to enhance the spectral efficiency for 5G and beyond cellular networks. Traditionally, D2D communication was considered solely as communication directly between two closely-located devices, without any support from the available network infrastructure; however, this understanding limits the advantages of D2D communication. Relay-assisted D2D communication was later proposed to allow devices to exchange data and extend coverage via relay strategy for transmission distance extension and capacity improvements. This work aims to determine the statistical quality-of-service (QoS) guarantees of a D2D link assisted by a full-duplex relay by employing a commonly used analytical tool, the effective capacity (EC). We provide a closed-form expression for the EC of relay-assisted D2D communication, in which both the transmitter and the relay devices operate under individual QoS constraints. We also provide an analysis of the impact of mode selection on the EC of relay-assisted D2D. Additionally, for the mode selection, we propose a novel multiple features-based mechanism by utilizing all the features of a wireless link. We further provide a closed-form solution for the non-convex calibration problem of the optimal weights for these underlying features. Finally, simulation results demonstrate how the quality of self-interference cancellation techniques impacts the EC of the relay-assisted D2D. The results also show that the performance of our proposed mode selection mechanism with optimal weights outperforms the traditional mode selection mechanism.

1 | INTRODUCTION

Cellular networks began to undergo rapid changes since the start of the twenty-first century. The fifth-generation (5G) cellular networks are already in the market, and the research on beyond 5G (B5G) networks is in full swing. The ever-increasing demands of higher data rates, low power consumption, and better quality-of-service (QoS) require unconventional thinking for B5G cellular networks. Device-to-device (D2D) communication can provide a solution for these demands by allowing two closely located devices to communicate without utilizing the cellular infrastructure.[1]

It also allows devices to reuse the cellular spectrum by transmitting with low power (to avoid interference); thus, has the potential to alleviate the spectrum scarcity problem of cellular networks. D2D communication is particularly beneficial for scenarios when communication through a base station (BS) is not possible or less efficient. However, it is challenging to set up a direct communication link between devices if they are not close by or the link conditions between them are not favorable.[2] Therefore, relying only on a direct D2D link may limit the advantages brought in by the D2D communication. In cases when a direct D2D link is not available, and the potential devices are on the periphery of the serving BS's coverage area, they need to leverage from an intermediate relay node to deliver data. This intermediate relay node can be another D2D/cellular user, a dedicated relay node deployed in the cell for relaying purposes, or a micro-cell BS (in a multi-tier cellular network scenario). Communication through an intermediate relay has many advantages, including but not limited to transmission distance extension and capacity improvements.[3]

The benefits of using intermediate relays in wireless networks brought the interests of the research industry into this direction. It leads to research into different aspects of relay-assisted communication such as uplink and downlink transmissions,[4,5] energy efficiency,[6] full-duplex (FD), and half-duplex (HD) relays,[7] etc. Moreover, the use of relays in D2D communication opens the door for various new research challenges as well as its potential as one of the key enabling technologies for B5G cellular networks. Relay-assisted D2D communication has been investigated in terms of relay selection techniques,[8-10] resource allocation,[11-13] transmission capacity enhancement,[14,15] etc. For instance, the authors in Reference 13 have proposed an energy-efficient resource allocation mechanism for D2D communication assisted by an FD relay. The main goal of this work is to maximize the energy efficiency of D2D users without influencing the QoS of the cellular users. On the other hand, Li et al[10] performs relay selection for assisting D2D communication based on the network level energy efficiency. The authors consider physical and social constraints to determine the best choice of relay devices. Another scheme[8] performs relay selection while considering end-to-end transmission delay, end-to-end data rate, and the battery life of the device. This work considers fixed-sized buffers (queues) at the transmitting and the relay devices. The simulation results show that the end-to-end delay increases as the buffer size and the average packet arrival rate increase in the proposed system model. Similarly, the authors in Reference 14 have performed a transmission capacity analysis of relay-assisted D2D communication in underlay and overlay transmission settings. The authors investigated different network and channel models to enhance the transmission capacity of the D2D link assisted by a relay. The works discussed above, and other similar research in the literature shows the importance and benefits of relay-assisted D2D communication. However, none of these works studies the impact of a relay on the QoS and reliability of the potential D2D link.

Relay-assisted D2D communication can only be integrated with B5G cellular networks once it provides the required reliability and QoS guarantees. Although the previously discussed studies provide significant insights for relay-assisted D2D communication, none of them study the impact of using a relay on the QoS and reliability of D2D communication. A relay-assisted D2D network must provide reliable and QoS-enabled communication for its potential use in various applications. To this end, some work performs the reliability and QoS analysis of D2D communication, such as References 16 and 17. They do not discuss scenarios where potential D2D pairs leverage intermediate relays for data transmission. One of the reasons is that it is challenging to ensure QoS guarantees of relay-assisted D2D communication due to its two-hop communication nature. Moreover, if both the transmitting and the relay device are resource-constrained devices (having finite transmission queues), there emerges a data backlog at both the devices due to the high packet drop ratio of the wireless link. This phenomenon consequently affects the overall QoS of the relay-assisted D2D communication. To this end, we provide a throughput analysis of D2D communication assisted by an FD relay under delay QoS constraints imposed at both the transmitting and the relay devices. We also note that because of the rapidly changing channel conditions, multipath fading, and mobility, the deterministic QoS guarantees are difficult (nearly impossible) to achieve.[18] Therefore, for our analysis, we use a well-known analytical tool: the effective capacity (EC), to find the statistical QoS guarantees.

The EC is an analytical tool to find the statistical QoS guarantees of a communication link. It is modeled in terms of the probability of having a non-empty queue and the delay violation probability. The EC can provide a maximum constant arrival rate at a transmitter's queue that can be supported by a time-varying departure process under the statistical QoS constraints.[19] The EC has attracted much interest due to its effectiveness and application in various settings of the networks. In References 20-22, authors have performed the EC analysis for cognitive radios. In References 23-25, it has been used to find the delay guarantees for non-orthogonal multiple access. The authors in References 26-28 have performed the EC analysis for relay networks and two-hop wireless networks. The authors in Reference 29 have performed the EC analysis for acoustic channel in underwater wireless sensor networks. More recently, the EC has also been used for statistical QoS guarantees for D2D communication.[16,17,30] In short, authors in Reference 31 have performed a detailed

survey on the EC analysis for different network settings. Although some works in the literature perform the EC analysis for D2D communication (as discussed earlier), to the best of the authors' knowledge, this work is the first of its kind that studies the statistical QoS guarantees of a D2D link assisted by an FD relay. The major contributions of this article can be summarized as follows:

- We propose a novel, multiple features-based mode selection (selection between direct and relay-assisted D2D modes) mechanism for D2D communication. It allows a transmit device to select a communication mode based on all the features of a wireless link, such as distance, path loss, SINR, RSSI, and channel capacity. This mechanism assigns weights to all the potential wireless channel features and makes a decision based on the optimal features. We also provide a closed-form solution for the non-convex calibration problem of the optimal weights for these underlying features.

- We consider two finite-sized queues in the network at both the transmitting and the relay device. We then perform the EC analysis by considering independent QoS guarantees at both of them. We also investigate the impact of the proposed mode selection mechanism on the EC analysis. Further, we compute the closed-form expression for the EC of an FD-enabled relay-assisted D2D communication.

- Based on the assumption that both the transmitting and the relay devices know the channel state information (CSI) before the transmission, we optimally allocate the transmission powers and transmission rates to both devices. The optimal transmission powers in each communication mode are calculated in such a way that minimizes the overall communication delay.

- Our numerical investigation shows that the mode selection, as well as the weight assignment to the features, have a strong impact on the EC of an FD-enabled relay-assisted D2D communication.

The remainder of this article has the following organization. Section 2 describes the system model and preliminaries. Section 3.1 presents multiple features-based mode selection. A closed-form solution for the non-convex calibration problem of the optimal weights for multiple features is also presented in Section 3.2. Section 4 presents the EC analysis of the FD-enabled relay-assisted D2D communication. Section 5 provides the simulation results. Finally, Section 6 concludes the article. TABLE 1 shows all the mathematical notations used in this article for the reader's convenience.

2 | SYSTEM MODEL AND PRELIMINARIES

2.1 | System model

The system model for D2D communication assisted by an FD relay is presented in Figure 1. We consider the region covered by a single cell and term the users present in the region as D2D users. When D2D user 1 (D_1) wants to communicate with D_2, it has to choose one of two available paths for communication: direct-D2D path ($D_1 \rightarrow D_2$) or relay-D2D path ($D_1 \rightarrow R \rightarrow D_2$). This problem of selecting between communication paths, which can also be considered as communication modes during every time-slot, is known as mode selection problem.[32] We will discuss this mode selection problem in detail in Section 3.

Further, we consider queues of length (steady state) Q_d and Q_r at D_1 and R, respectively. The QoS constraints at D_1 and R are θ_d and θ_r, respectively. We also consider $Z_1(k)$ and $Z_r(k)(Z_{r1}(k), Z_{r2}(k))$ as the magnitude square of the fading coefficients of the links $D_1 \rightarrow D_2$ and $D_1 \rightarrow R \rightarrow D_2$, respectively. Further, we note that the quality of a D2D wireless channel, which is defined by shadowing, multi-path fading, and inter-user and inter-channel interference, affects the achievable reliability. Prior knowledge of the channel conditions at the transmit D2D node plays an important role in achieving the required reliability. When the transmit D2D node has the perfect CSI before the transmission, it adjusts its transmission power and the transmission rate according to the channel conditions. This way, the optimal performance of the D2D channel can be achieved.[33] However, in practice, perfect knowledge of the CSI at the transmit D2D node is hard to acquire due to rapidly changing wireless channel conditions (slow and fast fading). Therefore, in practical wireless systems, block fading channel models are used. In these models, pilot bits are transmitted at the start of each fading/time block to approximate the fading process of the channel. This fading process is supposed to remain the same for the entire fading/time block. Therefore, we consider a block-fading channel whereby each block duration has constant fading and

TABLE 1 Mathematical notations

Notations	Description
$\mathbf{w}$	$\mathbf{w} = [w_1, \dots, w_N]^T$, set of weights for wireless channel features
m_{T_i}	Mean of test statistics T_i
$\mathbf{m}_T$	$\mathbf{m}_T = [m_{T_1}, \dots, m_{T_N}]^T$, mean vector of N features
σ_i^2	Variance of test statistics T_i
Q_d	Transmitter's queue length
Q_r	Relay's queue length
Q_T	Maximum tolerable queue length
θ_d	QoS exponent at transmitter's queue
θ_r	QoS exponent at relay's queue
r_a	Constant arrival rate at D_1
$r_d(k)$	Transmission rate of $D_1 \rightarrow D_2$ link
$r_r(k)$	Transmission rate of $D_1 \rightarrow R$ link
$C_{d_1,d_2}(k)$	Inst. channel capacity of $D_1 \rightarrow D_2$ link
$C_{d_1,r}(k)$	Inst. channel capacity of $D_1 \rightarrow R$ link
$C_{r,d_2}(k)$	Inst. channel capacity of $R \rightarrow D_2$ link
$\Lambda_{d_1,r}(\theta)$	Log. MGF of the channel capacity of $D_1 \rightarrow R$ link
$\Lambda_{r,d_2}(\theta)$	Log. MGF of the channel capacity of
$R \rightarrow D_2$ link	
$P_{d_1}^{\text{opt}}$	Optimal transmission power of D_1
P_r^{opt}	Optimal transmission power of R
$\gamma_d(k)$	SNR of $D_1 \rightarrow D_2$ link
$\gamma_{d_1,r}(k)$	SSINR of $D_1 \rightarrow R$ link
$\gamma_{r,d_2}(k)$	SNR of $R \rightarrow D_2$ link
ΔT_{pro}	Processing delay at R
$\Delta T_{d_1,d_2}$	Packet delay in direct-D2D mode
ΔT_r	Packet delay in relay-D2D mode
L	Length of data packet

fading changes independently between blocks. We also note that if the block length is long or the path loss changes rapidly (due to the user mobility), the fading approximation does not truly represent the entire fading/time block. We also assume that the perfect CSI is available at D_1 and R at the start of each fading block *. Thus, the service rate of the channels $D_1 \rightarrow D_2$, $D_1 \rightarrow R$, $R \rightarrow D_2$ are equal to their respective instantaneous channel capacities. D_1 and R use τ_1 and τ_2 time for transmission, respectively. Additionally, we assume that R operates in FD mode; thus, $\tau_1 + \tau_2 = 1$ time slot. A complete signal flow diagram is presented in Figure 2.

---

*When the transmitter is unaware of the CSI before the transmission or if the available CSI is imperfect, the analysis would change. The accuracy of the CSI at the transmitter can be characterized into; average SNR, perfect instantaneous SNR, and outdated instantaneous SNR. In an average SNR scenario, the transmitter is unaware of the instantaneous CSI but tracks the average SNR. Therefore, it schedules a packet of fixed size for each slot. In this scenario, the transmitted packets will be lost from time to time due to fading. In case the transmitter has perfect instantaneous CSI before transmission, it schedules packets of varying sizes per slot. In this scenario, packet loss is unlikely. On the other hand, if the transmitter has outdated instantaneous CSI and is aware of the imperfect CSI, it schedules packets of varying sizes. However, as the known CSI is not perfect, transmitted packets will be lost from time to time. This work only considers a scenario when perfect instantaneous CSI is available at the transmitter, and the remaining cases are out of scope. Interested readers are referred to[33] and[16] for the impact of imperfect and no CSI on the EC, respectively.
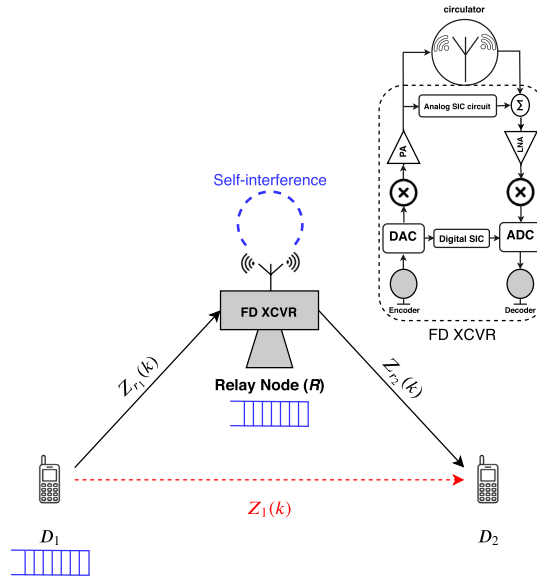
FIGURE 1 System model: the dotted arrow shows the direct-D2D link and the solid arrows represent relay-D2D link. D_1 can communicate with D_2 through either relay node link ($D_1 \rightarrow R \rightarrow D_2$) or direct link ($D_1 \rightarrow D_2$). Relay node ($R$) supports full duplex communication, while full duplex transceiver (FD XCVR) is also shown in the box which utilizes a shared antenna along with a circulator (to isolate self-interference)
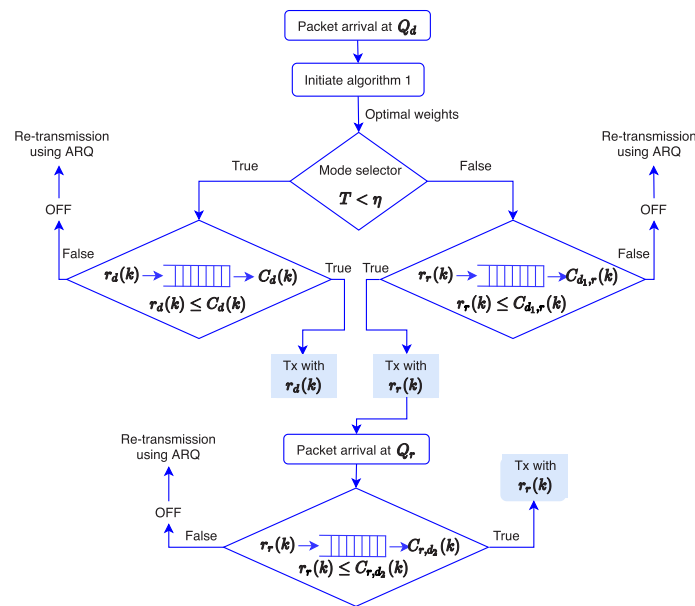

FIGURE 2 Flow diagram

2.2 | Full duplex (FD) relaying

FD communication is more efficient than the traditional way of half-duplex communication in terms of spectrum utilization as well as in energy consumption. Theoretically, FD can double the throughput of the communication link. It performs even better when used in shorter hops (with short link distance) because this way self-interference (SI) cancellation is much easier (due to small transmit power). However, if the inter-link distance becomes large then the FD transceiver will require high transmit power, which makes SI cancellation more challenging. Thus, it is more suitable to use FD enabled D2D communication when the network presents many shorter hops. One of the major caveats of FD

communication is SI, which is typically 70-90 dB stronger than that of the received signal, and it must be canceled-out for the received signal to be reconstructed successfully. Various SI cancellation techniques are available in the literature. For example, SI cancellation can be achieved through analog as well as digital cancellation.[34] Above that, antenna separation, antenna shielding, and beamforming can also be used for SI cancellation. The study in Reference 35 used two transmit antennas in such a way that both transmitted signals interfered destructively at the receive antenna. The authors in Reference 34 have proposed a Balun cancellation technique that requires only one transmit antenna and can also overcome the limitations of the previous schemes. The combination of analog and digital SI cancellation techniques can cancel 60-70 dB of the SI, which can be further enhanced by employing antenna array beamforming. However, even after incorporating all of these SI cancellation techniques, complete SI cancellation is not possible in practical FD systems. Therefore, we incorporate the residual SI in our analysis as a factor of noise.

3 | MULTIPLE FEATURES-BASED MODE SELECTION

The problem of mode selection at the transmitting device is basically choosing the best transmission path among a set of candidate paths. For the considered system model, mode selection implies selection between the direct-D2D path and the relay-assisted D2D path. Traditionally, the decision of mode selection is based on any feature of the wireless channel. For instance, the authors in Reference 36 use distance as a feature for selecting the best transmission path. Another study utilized path loss as a feature for mode selection.[16] The authors in Reference 37 provide a performance comparison between different mode selection strategies and design criteria. This comparison highlights that using a single wireless channel feature is not suitable for different network scenarios. For example, distance as a selection feature is not suitable for mode selection when the line-of-sight link is not available. Similarly, the path loss is only useful when the channel conditions are not changing rapidly. To address this issue, we propose a multiple features-based mode selection mechanism that considers all the wireless channel features (including but not limited to distance, path loss, RSSI, SINR, and channel capacity) for deciding the best transmission path. This mechanism assigns weights to these channel features, which are tunable according to the network conditions. Moreover, we provide Algorithm 1, which gives an optimal set of weights for any network condition.

3.1 | Binary hypothesis testing (BHT)

The mode selection problem at D_1 for each uplink transmission slot can be defined as the following BHT problem.

$$
\begin{cases}
H_0 : & \text{Direct-D2D mode } (D_1 \to D_2) \\
H_1 : & \text{Relay-D2D mode } (D_1 \to R \to D_2)
\end{cases}
\tag{1}
$$

Let $\hat{X}_i$ denote the noisy measurement of X_i, the ith feature, $i = 1, \ldots, N$. In this work, we assume that $\hat{X}_i \sim \mathcal{N}(X_i, \sigma_i^2)$, where σ_i^2 is the variance of estimation error. With multiple features in hand, two distinct approaches are plausible: (i) construct N binary hypothesis tests, one for each feature, and then combine/fuse the N binary outcomes in some heuristic way (eg, AND-ing, OR-ing, majority voting etc.) to make the ultimate decision about the transmission strategy; or (ii) construct a single BHT on a test statistic which is linear combination of the N measurements (of the features). For example, taking distance as a feature, a simple BHT could be constructed as follows: $d^{(D)} - d^{(R)} \underset{H_0}{\overset{H_1}{\gtrless}} 0$, where $d^{(D)}$ ($d^{(R)}$) is the distance between D_1 and D_2 (R). In general, one could write the following BHT: $T_i = \hat{X}_i^{(D)} - \hat{X}_i^{(R)} \underset{H_0}{\overset{H_1}{\gtrless}} 0$, for any feature i. Note that $T_i|H_0 \sim \mathcal{N}(-m_{T_i}, 2\sigma_i^2)$, and $T_i|H_1 \sim \mathcal{N}(m_{T_i}, 2\sigma_i^2)$, where $m_{T_i} = X_i^{(D)} - X_i^{(R)}$; without loss of generality, let $m_{T_i} > 0$ and denote $\mathbf{m}_T = [m_{T_1}, \ldots, m_{T_N}]^T$.

This work constructs a single BHT. Let $w_i > 0$ represent the weight assigned to feature X_i, $i = 1, \ldots, N$. Then, we propose the following test statistic: $T = \sum_{i=1}^{N} w_i T_i = \mathbf{w}^T \mathbf{T}$ where $\mathbf{w} = [w_1, \ldots, w_N]^T$, and $\mathbf{T} = [T_1, \ldots, T_N]^T$. Then, $T|H_0 \sim \mathcal{N}(-m_T, \sigma_T^2)$, and $T|H_1 \sim \mathcal{N}(m_T, \sigma_T^2)$, where $m_T = \sum_{i=1}^{N} w_i \cdot m_{T_i}$, and $\sigma_T^2 = 2\sum_{i=1}^{N} w_i^2 \sigma_i^2$.

Now by performing the log-likelihood ratio test, the mode selection mechanism for the uplink transmission is formulated as:[16]

$$LLR = \log_e\left(\frac{\mathbb{P}(T|H_1)}{\mathbb{P}(T|H_0)}\right) \underset{H_0}{\overset{H_1}{\gtrless}} \log_e\left(\frac{\pi(0)}{\pi(1)}\right) \Rightarrow T \underset{H_0}{\overset{H_1}{\gtrless}} \eta \tag{2}$$

where $\pi(0)$ and $\pi(1)$ are the prior probabilities of direct-D2D and relay-D2D modes, respectively, and $\eta = \log_e\left(\frac{\pi(0)}{\pi(1)}\right) \cdot \frac{\sum_{i=1}^{N} w_i^2 \sigma_i^2}{\sum_{i=1}^{N} w_i \cdot m_{T_i}}$. Note that $\log_e \delta = 0$ when the prior probabilities are equal. Consequently, $\eta = 0$, implying that BHT chooses the mode based on the sign of T, the test statistic.

3.2 | Performance of the BHT

To measure the performance of the BHT, we use correct detection ($\mathbb{P}(H_0|H_0)$ and $\mathbb{P}(H_1|H_1)$)and error ($\mathbb{P}(H_1|H_0)$ and $\mathbb{P}(H_0|H_1)$)probabilities. Moreover, to find the reliability of the feature measurement as well as the BHT problem, we use the Kullback-Leibler divergence (KLD).

The probability of correct detection of H_0 is given as:

$$P_{d,1} = \mathbb{P}(H_0|H_0) = \mathbb{P}(T < \eta|H_0) = 1 - Q\left(\frac{\eta + m_T}{\sigma_T}\right) \tag{3}$$

where $Q(x)$ is a Marcum Q-function. $P_{d,1}$ represents the correct-detection probability of selecting the direct-D2D mode. It shows that the direct-D2D transmission path was the best among the candidate paths and the multiple features-based mode selection mechanism also detects the direct-D2D path. On the other hand, when the direct-D2D path is the best path but the mode selection mechanism makes an error and selects the relay-D2D transmission path, there occurs a mode selection error. This error can be calculated by the type-I error probability ($P_{e,1}$), which is as follows:

$$P_{e,1} = \mathbb{P}(H_1|H_0) = \mathbb{P}(T > \eta|H_0) = Q\left(\frac{\eta + m_T}{\sigma_T}\right) \tag{4}$$

Similarly, the correct detection probability for selecting the relay-D2D path is given as:

$$P_{d,2} = \mathbb{P}(H_1|H_1) = \mathbb{P}(T > \eta|H_1) = Q\left(\frac{\eta - m_T}{\sigma_T}\right). \tag{5}$$

And the probability of type-II error (when the relay-D2D path was the best but the mode selection mechanism erroneously select the direct-D2D path) is given as:

$$P_{e,2} = \mathbb{P}(H_0|H_1) = \mathbb{P}(T < \eta|H_1) = 1 - Q\left(\frac{\eta - m_T}{\sigma_T}\right) \tag{6}$$

The KLD is defined as[†]:

$$D(\mathbb{P}(T|H_1)||\mathbb{P}(T|H_0)) = \int_{-\infty}^{\infty} \mathbb{P}(T|H_1)\log\left(\frac{\mathbb{P}(T|H_1)}{\mathbb{P}(T|H_0)}\right)dT \tag{7}$$

In our case, KLD comes out to be as follows:

$$D(\mathbb{P}(T|H_1)||\mathbb{P}(T|H_0)) = \frac{m_T^2}{\sigma_T^2} = \frac{\mathbf{w}^T \Omega_m \mathbf{w}}{\mathbf{w}^T \Lambda_{\sigma^2} \mathbf{w}} \tag{8}$$

where Ω_m denotes an $N \times N$ matrix and equals $\mathbf{m}_T \mathbf{m}_T^T$ and $\Lambda_{\sigma^2} = \begin{bmatrix} \sigma_1^2 & & \\ & \ddots & \\ & & \sigma_N^2 \end{bmatrix}$

[†]In general, Jensen-Shannon divergence (JSD) should be preferred over KLD because JSD is a true distance measure, while KLD is not. However, in our case, we have enough symmetry such that $D(\mathbb{P}(T|H_1)||\mathbb{P}(T|H_0)) = D(\mathbb{P}(T|H_0)||\mathbb{P}(T|H_1))$, so it suffices to use KLD.

We now find the optimal set of weights $\{w_i\}_{i=1}^{N}$ which maximizes the KLD (which in turn minimizes both $P_{e,1}$ and $P_{e,2}$ simultaneously). The optimization problem is given as:

$$\max_{\{w_i\}_{i=1}^{N}} f(\mathbf{w}) = D(\mathbb{P}(T|H_1)||\mathbb{P}(T|H_0)) = \frac{\mathbf{w}^T \Omega_m \mathbf{w}}{\mathbf{w}^T \Lambda_{\sigma^2} \mathbf{w}}$$

Subject to: $w_i > 0, \forall i \in (i, \ldots, N)$

$$|\mathbf{w}| = \sum_{i=1}^{N} w_i = 1 \tag{9}$$

Lemma 1. *The optimization problem in (9) is a non-convex problem.*

Proof. See Appendix A. ∎

The solution in (9) is an NP-hard problem,[38] and we try to solve it using augmented Lagrangian method and alternative direction multiplier method (ADMM).

Beforehand, the problem in (9) could recast as

$$\max_{t,\{w_i\}_{i=1}^{N}} t$$

Subject to: $t > 0, w_i > 0, \forall i \in (i, \ldots, N)$

$$\left\| \Omega_m^{\frac{1}{2}} \mathbf{w} \right\| = t \left\| \Lambda_{\sigma^2}^{\frac{1}{2}} \mathbf{w} \right\|$$

$$|\mathbf{w}| = \sum_{i=1}^{N} w_i = 1 \tag{10}$$

We moved the constraints into the objective function, resulting in the corresponding, augmented Lagrangian problem:

$$\max_{t,\{w_i\}_{i=1}^{N}} t - \mu \left\{ \left\| \Omega_m^{\frac{1}{2}} \mathbf{w} \right\| - t \left\| \Lambda_{\sigma^2}^{\frac{1}{2}} \mathbf{w} \right\| \right\}^2$$

Subject to: $t > 0, w_i > 0, \forall i \in (i, \ldots, N)$

$$|\mathbf{w}| = \sum_{i=1}^{N} w_i = 1 \tag{11}$$

where μ is a penalty parameter.

For the problem in (11), we can split it into a t-subproblem and a $\mathbf{w}$-subproblem.

- The t-subproblem can be compactly rewritten as

$$\max_{t}\{t - \mu(a - tb)^2\}$$

$$= -\mu b^2 t^2 + (1 + 2\mu ab)t - \mu a^2$$

Subject to: $t > 0 \tag{12}$

where $a = \left\| \Omega_m^{\frac{1}{2}} \mathbf{w} \right\|$ and $b = \left\| \Lambda_{\sigma^2}^{\frac{1}{2}} \mathbf{w} \right\|$. We have

$$t^{\text{opt}} = \max \left\{ \frac{1 + 2\mu ab}{2\mu b^2}, 0 \right\} \tag{13}$$

- The $\mathbf{w}$-subproblem can be formulated as

$$\min_{\{w_i\}_{i=1}^{N}} v(\mathbf{w}) = \left\{ \left\| \Omega_m^{\frac{1}{2}} \mathbf{w} \right\| - t \left\| \Lambda_{\sigma^2}^{\frac{1}{2}} \mathbf{w} \right\| \right\}^2$$

$$= \mathbf{w}^T \Omega_m \mathbf{w} + t^2 \mathbf{w} \Lambda_{\sigma^2} \mathbf{w} - 2t \left\| \Omega_m^{\frac{1}{2}} \mathbf{w} \right\| \left\| \Lambda_{\sigma^2}^{\frac{1}{2}} \mathbf{w} \right\|$$

Subject to: $w_i > 0, \forall i \in (i, \dots, N)$

$$|\mathbf{w}| = \sum_{i=1}^{N} w_i = 1 \qquad (14)$$

We attempt to find a locally tight upper-bound for $\nu(\mathbf{w})$ rather than minimizing $\nu(\mathbf{w})$, and have the following Lemma.

Lemma 2. *The minimization of $\nu(\mathbf{w})$ could be upper bounded by the minimization of the problem in (15), where $\tilde{\mathbf{w}}$ as an approximation of $\mathbf{w}$ at a previous iteration and λ_w denotes a Lagrangian factor.*

Proof. See Appendix B. ∎

$$\mathcal{L}(\mathbf{w}, \lambda_w) = \min_{\{w_i\}_{i=1}^{N}} \mathbf{w}^T \left\{ \Omega_m + t^2 \Lambda_{\sigma^2} - t \frac{\Lambda_{\sigma^2} \tilde{\mathbf{w}} \tilde{\mathbf{w}}^T \Omega_m + \Omega_m \tilde{\mathbf{w}} \tilde{\mathbf{w}}^T \Lambda_{\sigma^2}}{\left\| \Omega_m^{\frac{1}{2}} \tilde{\mathbf{w}} \right\| \left\| \Lambda_{\sigma^2}^{\frac{1}{2}} \tilde{\mathbf{w}} \right\|} \right\} \mathbf{w} + \lambda_w \left(\sum_{i=1}^{N} w_i - 1 \right) \qquad (15)$$

For simplicity of representation, we define an augmented vector $\mathbf{w}_{\text{aug}} = [\mathbf{w}; \lambda_w]$; a matrix $\Gamma = \Omega_m + t^2 \Lambda_{\sigma^2} - t \frac{\Lambda_{\sigma^2} \tilde{\mathbf{w}} \tilde{\mathbf{w}}^T \Omega_m + \Omega_m \tilde{\mathbf{w}} \tilde{\mathbf{w}}^T \Lambda_{\sigma^2}}{\left\| \Omega_m^{\frac{1}{2}} \tilde{\mathbf{w}} \right\| \left\| \Lambda_{\sigma^2}^{\frac{1}{2}} \tilde{\mathbf{w}} \right\|}$; an augmented matrix $\Gamma_{\text{aug}} = \begin{bmatrix} \Gamma & \mathbf{1} \\ \mathbf{1}^T & 0 \end{bmatrix}$; and an $(N+1)$-length vector $\mathbf{y} = [0; \dots; 0; 1]$. Given the symmetry of Γ, we could have $\mathbf{w}_{\text{aug}}^{\text{opt}} = \Gamma_{\text{aug}}^{-1} \mathbf{y}$. Thus, the values of $\mathbf{w}$ could be easily obtained from $\mathbf{w}_{\text{aug}}$ as $\mathbf{w} = \max\{\mathbf{w}_{\text{aug}} (1 : N), 0\}$.

In summary, the optimization problem in (9) could be solved by iteratively processing the t-subproblem and $\mathbf{w}$-subproblem. The whole procedure is summarized in Algorithm 1. This algorithm provides the optimal set of weights for the underlying wireless channel features. These optimal weights are then used in the multiple features-based mode selection mechanism to find the best communication modes for data transmission in different network settings. The computational complexity of Algorithm 1 is $O(N^3)$ [‡]. The convergence of Algorithm 1 has been proved and provided in Appendix C.

Algorithm 1. The optimization of $\mathbf{w}$

---

initialize $\mathbf{w}$, μ and t

repeat

   Update a and b as $a \leftarrow \left\| \Omega_m^{\frac{1}{2}} \mathbf{w} \right\|$ and $b \leftarrow \left\| \Lambda_{\sigma^2}^{\frac{1}{2}} \mathbf{w} \right\|$.

   Update t by $t \leftarrow \max \left\{ \frac{1 + 2\mu ab}{2\mu b^2}, 0 \right\}$.

   Update $\tilde{\mathbf{w}}$ by $\tilde{\mathbf{w}} \leftarrow \mathbf{w}$.

   Update $\mathbf{w}$ based on $\mathbf{w}_{\text{aug}} \leftarrow \Gamma_{\text{aug}}^{-1} \mathbf{y}$.

until $\|\mathbf{w} - \tilde{\mathbf{w}}\|$ is smaller than a predefined threshold.

Next, we perform the EC analysis of D2D communication assisted by an FD relay. We also investigate the impact of the proposed multiple features-based mode selection on the EC analysis.

4 | EC ANALYSIS OF RELAY-ASSISTED D2D COMMUNICATION

In the relay-assisted D2D communication scenario, where there are two finite-sized queues in the network, the QoS exponents θ_d and θ_r can be defined as,

---

[‡]Computing a and b involves $O(N^2)$ and $O(N)$ multiplications, respectively. Computing t involves $O(1)$ multiplications. Computing Γ needs another $O(N^2)$ multiplications and the inverse of Γ takes $O(N^3)$ multiplications, which is also most computation-intense. The update of $\mathbf{w}_{\text{aug}}$ requires $O(N)$ multiplications. In summary, the computational complexity of Algorithm 1 is bounded by $O(N^3)$.

$$\lim_{Q_T \to \infty} \frac{\log \mathbb{P}[Q_d > Q_T]}{Q_T} = -\theta_d$$

$$\lim_{Q_T \to \infty} \frac{\log \mathbb{P}[Q_r > Q_T]}{Q_T} = -\theta_r \tag{16}$$

where Q_T is the maximum tolerable queue length. If (16) satisfies, then the queue violation probability at D_1 and R for large Q_T becomes,

$$\mathbb{P}[Q_d \geq Q_T] \approx e^{-\theta_d Q_T}$$

$$\mathbb{P}[Q_r \geq Q_T] \approx e^{-\theta_r Q_T} \tag{17}$$

From (17), we can say that θ_d and θ_r are the exponential decay rates of the queue overflow probabilities at D_1 and R, respectively. We also observe that low θ_d and θ_r yield a higher queue overflow probability. This entails relaxed QoS constraints at D_1 and R. Contrarily, large θ_d and θ_r refer to a low queue overflow probability. This ultimately results in more strict QoS constraints at D_1 and R. In short, when θ_d and θ_r approach zero, it implies delay-tolerant communication, and when θ_d and (θ_r) approach infinity, it implies delay-limited communication.

The EC of a point-to-point (P2P) link is defined by Wu et al in Reference 19, which states that,

$$EC = -\frac{\Lambda(-\theta)}{\theta} = -\lim_{t \to \infty} \frac{1}{\theta t} \log \mathbb{E}(e^{-S(t)\theta}) \tag{18}$$

where $S(t)$ is the service process rate of the queue. In the case of a D2D link assisted by an FD relay with individual delay constraints at both the transmitter and the relay, there become two P2P links. One P2P link is from $D_1 \to R$ and the second P2P link is from $R \to D_2$. Therefore, there will be a separate EC at D_1 and R, which can be written as,

$$EC_{D_1} = -\frac{\Lambda(-\theta_d)}{\theta_d} = -\lim_{t \to \infty} \frac{1}{\theta_d t} \log \mathbb{E}(e^{-S_1(t)\theta_d})$$

$$EC_R = -\frac{\Lambda(-\theta_r)}{\theta_r} = -\lim_{t \to \infty} \frac{1}{\theta_r t} \log \mathbb{E}(e^{-S_2(t)\theta_r}) \tag{19}$$

where $S_1(t)$ and $S_2(t)$ are the service process rate of Q_d and Q_r, respectively. To determine the overall EC of this cascaded network, we utilize the results from the EC of two-hop wireless link.[26] Thus, the overall EC of relay-assisted D2D link becomes,

$$EC_{D_2}^{D_1}(\theta_d, \theta_r) = \sup_{EC \varepsilon \mathbf{EC}} EC \tag{20}$$

where $\mathbf{EC}$ is a collection of EC_{D_1} and EC_R.

To satisfying the QoS constraints for the relay-assisted D2D link, we assume that the constant arrival rate at D_1 is always greater than zero ($r_a \geq 0$). We also assume that all the communication links use their corresponding instantaneous channel capacities for transmission. In order to satisfy the QoS constraints at D_1, we must have $\overline{\theta} \geq \theta_d$, where $\overline{\theta}$ is the solution to

$$r_a = -\frac{\Lambda_{d_1,r}(-\overline{\theta})}{\overline{\theta}} \tag{21}$$

and $\Lambda_{d_1,r}$ is the log moment generating function (log-MGF) of the channel capacity of $D_1 \to R$ link. Now to find the log-MGF at R, we utilize results from the principles of Effective Bandwidth.[39] We know that the log-MGF of the departure process at D_1 is equal to the log-MGF of the arrival process at R. Therefore, we can write the log-MGF of the arrival process at $R(\Lambda_r(\theta))$ for different values of θ as follows:

$$\Lambda_r(\theta) = \begin{cases} r_a \theta, & 0 \leq \theta \leq \overline{\theta} \\ r_a \overline{\theta} + \Lambda_{d_1,r}(\theta - \overline{\theta}), & \theta > \overline{\theta}. \end{cases} \tag{22}$$

Similarly, for satisfying the QoS constraints at R, we must have $\hat{\theta} \geq \theta_r$, where $\hat{\theta}$ is the solution to Reference 39,

$$\Lambda_r(\hat{\theta}) + \Lambda_{r,d_2}(-\hat{\theta}) = 0 \tag{23}$$

and where $\Lambda_{r,d_2}(-\hat{\theta})$ is log-MGF of the channel capacity of the $R \rightarrow D_2$ link.

To find EC_{D_1} and EC_R, we need to find the instantaneous channel capacities of the respective links. We find these capacities in the next section.

4.1 | Transmit power optimization

In our analysis, we assume that D_1 and R have perfect CSI of their respective channels. Therefore, D_1 and R will adjust their transmission rates and transmit powers based on the channel conditions. Let $C_d(k)$ and $C_r(k)$ represent the instantaneous channel capacities (bits/sec) of the links $D_1 \rightarrow D_2$ and $D_1 \rightarrow R \rightarrow D_2$ in time slot k, respectively. Before computing these capacities, we note that R works in the FD mode; thus, a SI will be introduced at R. Although a major portion of SI can be neutralized by employing various analog and digital SI cancellation techniques (see Section 2.2), complete SI cancellation is not possible in practical FD systems. Therefore, we incorporate the residual SI in the SINR of the relay-D2D link to nullify its effect on the channel capacity of the relay link. The distribution of residual SI cannot be known in practice after multiple stages of SI cancellation. However, we consider a worst-case scenario where its distribution is modeled as Gaussian ($I \sim \mathcal{N}(0, \sigma_{si})$). It has zero-mean and variance $\sigma_{si} = \alpha P_r^{\beta}$,[40] where α and $\beta (0 \leq \beta \leq 1)$ are constants and reflect the quality of the SI cancellation techniques used and P_r is the transmit power of the relay node. We calculate the instantaneous channel capacities from the following equations.

$$C_{d_1,d_2}(k) = B\log_2\left(1 + \frac{P_{d_1}^{\text{opt}} Z_1(k)}{PL_{d_1,r} N_o}\right) = B\log_2(1 + \gamma_d(k)) \tag{24}$$

$$C_r(k) = \min\{C_{d_1,r}(k), C_{r,d_2}(k)\}$$

$$= B\log_2\left(1 + \min\left\{\frac{P_{d_1}^{\text{opt}} Z_{r_1}(k)}{PL_{d_1,r} N_o + \alpha P_r^{\text{opt}\beta}}, \frac{P_r^{\text{opt}} Z_{r_2}(k)}{PL_{r,d_2} N_o}\right\}\right)$$

$$= B\log_2\left(1 + \min\left\{\frac{P_{d_1}^{\text{opt}} Z_{r_1}(k)}{1 + \overline{\alpha} P_r^{\text{opt}\beta}}, \frac{P_r^{\text{opt}} Z_{r_1}(k)}{PL_{r,d_2} N_o}\right\}\right)$$

$$= B\log_2(1 + \min\{\gamma_{d_1,r}(k), \gamma_{r,d_2}(k)\})$$

$$= B\log_2(1 + \gamma_r(k)) \tag{25}$$

where $\gamma_d(k)$ and $\gamma_r(k) = \min\{\gamma_{d_1,r}(k), \gamma_{r,d_2}(k)\}$ are the net SINR of the direct-D2D ($D_1 \rightarrow D_2$) and relay-D2D ($D_1 \rightarrow R \rightarrow D_2$) links, respectively; $PL_{d_1,r}$ and PL_{r,d_2} are the pathloss between $D_1 \rightarrow R$ and $R \rightarrow D_2$, respectively; $Z_1(k)$, $Z_{r_1}(k)$, and $Z_{r_2}(k)$ are the magnitude square of the fading coefficients between $D_1 \rightarrow D_2$, $D_1 \rightarrow R$, and $R \rightarrow D_2$, respectively; N_0 is the noise variance at R; B is the bandwidth; $\overline{\alpha} = \frac{\alpha}{PL_{d_1,r} N_o}$; and $P_{d_1}^{\text{opt}}$ and P_r^{opt} are the optimal transmit powers of the D_1 and R, respectively. We will select $P_{d_1}^{\text{opt}}$ and P_r^{opt} in such a way that they will minimize the delay to transmit a packet in their respective communication modes. Moreover, $\overline{\alpha} P_r^{\text{opt}\beta}$ is the self-interference-to-noise-ratio (INR) for FD relaying at R. One can write the transmission rates $r_d(k)$ and $r_r(k)$ as $r_d(k) = B\log_2(1 + \gamma_d(k))$ and $r_r(k) = B\log_2(1 + \gamma_{d_1,r}(k))$. We now compute the optimal transmission power ($P_{d_1}^{\text{opt}}, P_r^{\text{opt}}$) in each communication modes.

4.1.1 | Direct-D2D mode

Packet delay in direct-D2D mode can be calculated as

$$\Delta T_d = \Delta T_{d_1,d_2} = \frac{L}{C_{d_1,d_2}(k)} = \frac{L}{B\log_2\left(1 + \frac{P_{d_1} Z_1(k)}{PL_{d_1,d_2} N_0}\right)} \tag{26}$$

where L is the length of data packet to be transmitted. We assume that when packet L arrives at the transmission queue Q_d, the queue is empty. Therefore, no delay occurs at Q_d. In this mode we select optimal P_{d_1} ($P_{d_1}^{opt}$) by minimizing ΔT_d. So, the optimization problem would become,

$$\min_{P_{d_1}} \left\{ \frac{L}{B \log_2 \left(1 + \frac{P_{d_1} Z_1(k)}{PL_{d_1,d_2} N_o} \right)} \right\} \text{ subject to: } 0 \le P_{d_1} \le P_{d_1}^{max} \tag{27}$$

It is obvious that $P_{d_1}^{opt} = P_{d_1}^{max}$ yields the minimum of ΔT_d solution.

4.1.2 | Relay-D2D mode

Packet delay in relay-D2D mode can be calculated as

$$\Delta T_r = \Delta T_{d_1,r} + \Delta T_{pro} + \Delta T_{r,d_2}$$
$$= \frac{L}{C_{d_1,r}(k)} + \Delta T_{pro} + \frac{L}{C_{r,d_2}(k)} \tag{28}$$

where $C_{d_1,r}(k) = B \log_2(1 + \frac{P_{d_1} Z_{r_1}(k)}{PL_{d_1,r} N_0 + \alpha P_r^{opt\beta}})$ and $C_{r,d_2}(k) = B \log_2(1 + \frac{P_r Z_{r_2}(k)}{PL_{r,d_2} N_0})$ are the channel capacities of $D_1 \to R$ and $R \to D_2$ links, respectively. ΔT_{pro} is the processing delay at R and it depends on the data forwarding scheme being used at the relay. For instance, ΔT_{pro} will be greater for the decode and forward operation than for the amplify and forward operation. ΔT_{pro} is a nuisance parameter (ie, the control/design variables/transmit powers have no influence over it), and thus it can be dropped from the optimization problem. In this mode we have to find the optimal P_{d_1} ($P_{d_1}^{opt}$) and optimal P_r (P_r^{opt}) in such a way that minimizes ΔT_r. So, the optimization problem would become,

$$\min_{P_{d_1}, P_r} \left\{ \frac{L}{B \log_2 \left(1 + \frac{P_{d_1} Z_{r_1}(k)}{PL_{d_1,r} N_0 + \alpha P_r^\beta} \right)} + \frac{L}{B \log_2 \left(1 + \frac{P_r Z_{r_2}(k)}{PL_{r,d_2} N_0} \right)} \right\}. \tag{29}$$

$$\text{subject to: } \begin{array}{l} 0 \le P_{d_1} \le P_{d_1}^{max} \\ 0 \le P_r \le P_r^{max} \\ C_{d_1,r}(k) \le C_{r,d_2}(k) \end{array}$$

The constraint in (29) is due to the fact that if $C_{d_1,r}(k) > C_{r,d_2}(k)$, there will emerge increasingly longer queue at the relay node, possibly incurring packet drop and infinite delay. Moreover, for a queuing system to be stable, the $R \to D_2$ link's average transmission rate should be greater than the $D_1 \to R$ link's average transmission rate.[39] Therefore, in this work, we limit our scope to the scenario with the constraint in (29). As for the solutions, we have

- Similar to the optimization of ΔT_d, $P_{d_1}^{opt} = P_{d_1}^{max}$ yields the minimum ΔT_r solution.
- On the other hand, after considering the constraint in (29), P_r^{opt} could be approximated by relaxing the problem (29) to

$$\min_{P_{d_1}, P_r} \left\{ \frac{L}{C_{d_1,r}(k)} \right\}, \text{ subject to: } \begin{array}{l} P_{d_1} = P_{d_1}^{max} \\ 0 \le P_r \le P_r^{max} \\ C_{d_1,r}(k) \le C_{r,d_2}(k) \end{array} \tag{30}$$
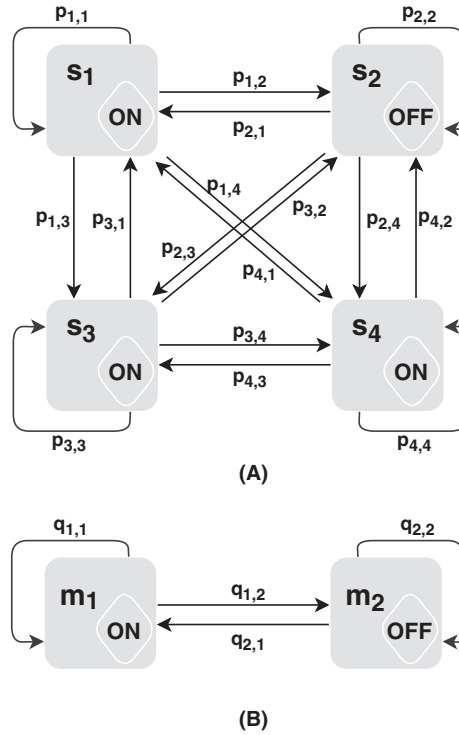
FIGURE 3 A, State diagram at D_1, which is modeled as a Markovian system with $M = 4$ states; B, State diagram at R, which is modeled as a Markovian system with $M = 2$ states

The minimum is obtained when $C_{d_1,r}(k) = C_{r,d_2}(k)$ or $P_r^{\text{opt}} Z_{r_2}(k)(PL_{d_1,r}N_o + \alpha P_r^{\text{opt}}) = PL_{r,d_2} N_o P_{d_1} Z_{r_1}(k)$ for $0 \leq P_r^{\text{opt}} \leq P_r^{\text{max}}$. In other words,

$$P_r^{\text{opt}} = \min \left\{ P_r^{\text{max}}, \sqrt{\frac{PL_{r,d_2}N_o P_{d_1} Z_{r_1}(k)}{\alpha Z_{r_2}(k)} + \frac{(PL_{d_1,r}N_o)^2}{4\alpha^2} - \frac{PL_{d_1,r}N_o}{2\alpha}} \right\} \tag{31}$$

The transmitting device (D_1) and the relay node (R) transmits using the above-calculated optimal transmission rates in direct-D2D and relay-D2D modes. This fact combined with the mode selection makes the D2D channel a Markov service process. Next, we perform Markov chain modeling of the D2D link.

4.2 | Markov chain modeling

Based on the mode selection and adaptive transmission rate, a four-state Markov process has been established at D_1, as shown in Figure 3A and explained in Table 2. When direct-D2D mode is selected (as in states s_1 and s_3), the transmission rate $r_d(k)$ is either equal (in s_1) or less (in s_3) than the instantaneous channel capacity. In both of the scenarios, reliable communication is attained at the rate of $r_d(k)$; thus, both of these states are in ON condition. When the relay-D2D mode is selected (as in states s_2 and s_4), the transmission rate $r_r(k)$ is greater than the instantaneous channel capacity in s_2 §; thus, the successful transmission is not possible, and it is considered as an OFF state. For the state s_4, the transmission rate $r_r(k)$ is equal to the instantaneous channel capacity; thus, the successful transmission attained at $r_r(k)$, and it is considered as ON state.

---

§This is due to the assumption that in the direct-D2D mode, channel reuse policy is used for uplink transmission, whereas, a dedicated channel is allocated in case of relay-D2D. Therefore, the transmitter does not consider the interference caused by the cellular user.[20]

TABLE 2 Markov chain representation of four states

State	Description	Notation	Action
s_1	Direct D2D mode is selected and the link is ON	H_0/H_0 & $r_d(k) = C_{d_1,d_2}(k)$	Reliable communication is attained at the rate of $r_d(k)$
s_2	Relay D2D mode is selected and the link is OFF	H_1/H_0 & $r_r(k) > C_{d_1,d_2}(k)$	No transmission
s_3	Direct D2D mode is selected and the link is ON	H_0/H_1 & $r_d(k) < C_{d_1,r}(k)$	Reliable communication is attained at the rate of $r_d(k)$
s_4	Relay D2D mode is selected and the link is ON	H_1/H_1 & $r_r(k) = C_{d_1,r}(k)$	Reliable communication is attained at the rate of $r_r(k)$

For states s_1, s_2, s_3, and s_4, as shown in Figure 3A, there emerges a transition probability matrix (**P**) at D_1. Now we find entries of the matrix (**P**). Note that when D_1 has perfect CSI, the transmission rate in each state becomes a random process. Therefore, the state transition probabilities rely solely on the detection probabilities and on the prior probabilities of the direct-D2D and the relay-D2D modes:

$$p_{i1} = p_1 = \pi_0 P_{d,1} = \pi_0 \mathbb{P}(T < \eta|H_0) = 1 - Q\left(\frac{\eta + m_T}{\sigma_T}\right)$$

$$p_{i2} = p_2 = \pi_0 P_{e,1} = \pi_0 \mathbb{P}(T > \eta|H_0) = Q\left(\frac{\eta + m_T}{\sigma_T}\right)$$

$$p_{i3} = p_3 = \pi_1 P_{e,2} = \pi_1 \mathbb{P}(T < \eta|H_1) = 1 - Q\left(\frac{\eta - m_T}{\sigma_T}\right)$$

$$p_{i4} = p_4 = \pi_1 P_{d,2} = \pi_1 \mathbb{P}(T > \eta|H_1) = Q\left(\frac{\eta - m_T}{\sigma_T}\right) \tag{32}$$

From (32), each row of **P** becomes $[p_1, p_2, p_3, p_4]$. Due to identical rows, **P** has rank 1.

On the other hand, due to the presence of another queue in the network, a decision has to be taken at R for the successful transmission. If the arrival rate at the queue of R is less or equal to the instantaneous channel capacity of $R \rightarrow D_2$ link, then the successful transmission is possible at $r_r(k)$. Otherwise, there emerges an increasingly longer queue at R, which can possibly incur infinite delay; thus, the successful transmission is not possible at the steady-state position. Based on this, there emerge the following two states:

m_1: $r_r(k) > C_{r,d_2}(k) \Rightarrow$ OFF,

m_2: $r_r(k) \leq C_{r,d_2}(k) \Rightarrow$ ON,

where $r_r(k)$ is the arrival rate at R, which equals the service rate of D_1 (in relay-D2D mode) and the instantaneous channel capacity of $D_1 \rightarrow R$ link ($C_{d_1,r}$). $C_{r,d_2}(k)$ is the instantaneous channel capacity of the link $R \rightarrow D_2$. For the states m_1 and m_2, depicted in Figure 3B, the state transition probability matrix **Q** would be

$$\mathbf{Q} = \begin{bmatrix} q_{1,1} & q_{1,2} \\ q_{2,1} & q_{2,2} \end{bmatrix} = \begin{bmatrix} q_1 & q_2 \\ q_1 & q_2 \end{bmatrix} \tag{33}$$

Note that, due to identical rows, **Q** also has rank 1.

We now use the results of Markov chain modeling at D_1 and R and combine them with the mode selection to find the EC of relay-assisted D2D communication.

4.3 | EC of relay-assisted D2D link

To find the final expression for the EC of relay-assisted D2D link, we now find the closed-form expressions of EC_{D_1} and EC_R, and for that we have the following two Lemmas.

Lemma 3. *The EC at D_1 is given by the following:*

$$EC_{D_1} = -\frac{1}{\theta_d} \log_e \left((p_1 + p_3)\mathbb{E}_{z_1}[e^{-r_d(k)\theta_d}] + p_2 + p_4 \mathbb{E}_{z_{r1}}[e^{-r_r(k)\theta_d}]\right) \tag{34}$$
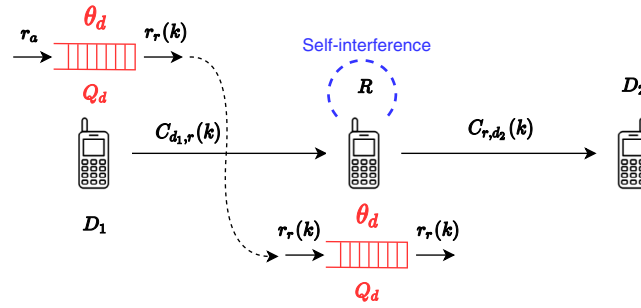
FIGURE 4 Relay-assisted D2D communication network: D_1, R, and D_2 are the transmitter, relay, and receiver devices, respectively. Q_d, θ_d and Q_r, θ_r are the steady-state queue length and QoS exponent for the D_1 and R, respectively. $C_{d_1,r}$ and C_{r,d_2} are the instantaneous channel capacities of the links $D_1 \rightarrow R$ and $R \rightarrow D_2$, respectively.

Proof. See Appendix D. ∎

Lemma 4. *The EC at R is given by the following:*

$$EC_R = -\frac{1}{\theta_r} \log_e \left(q_1 \mathbb{E}_{z_{r2}}[e^{-C_{r,d_2}(k)\theta_r}] + q_2 \right) \tag{35}$$

Proof. See Appendix E. ∎

By substituting results from (34) and (35) in (20), we can find the final expression for the EC of a D2D link assisted by an FD relay. Note that for a two-queue system (as shown in Figure 4) to be stable, the average transmission rate of $D_1 \rightarrow R$ must be less than that of the $R \rightarrow D_2$ link. Therefore, we assume that the condition $\mathbb{E}_{z_{r1}}\{\log_2(1 + \gamma_{d_1,r}Z_{r1})\} < \mathbb{E}_{z_{r2}}\{\log_2(1 + \gamma_{r,d_2}Z_{r_2})\}$ is satisfied. Further, we observe that different QoS constraints on the transmitter and the relay node queues affect the overall EC of relay-D2D link. To provide a comprehensive analysis, we additionally explore some of the conditions on the QoS constraints for the relay-D2D link. These conditions define the EC of relay-D2D link in different scenarios, such as when the transmitter's queue operates under more strict delay constraints than the relay node's queue and vice versa. These conditions and their respective ECs are provided in the Appendix F.

Remark 1. Bound on the Constant Arrival Rate at D_1:

D2D communication assisted by an FD relay under QoS constraints θ_d and θ_r can support a constant arrival rate (r_a) at the transmitter's queue. We say that r_a is upper bounded by $\min\{EC_{D_1}, EC_R\}$. To prove this bound, we first investigate r_a at D_1. We know from (21) that $r_a = EC_{D_1}(\bar{\theta})$ and $EC_{D_1}(\bar{\theta}) \leq EC_{D_1}(\theta_d)$ for any $\bar{\theta}$ as long as $\bar{\theta} \geq \theta_d$. From here, we can see that the maximum value $EC_{D_1}(\bar{\theta})$ can get is $EC_{D_1}(\theta_d)$, and so does r_a. On the other hand, if we assume that there is no queue at D_1 and hence r_a is transmitted without any delay then the service rate of D_1 becomes r_a. We know that the service rate of D_1 is equal to the arrival rate at R, which in this case will be a constant value of r_a rather than a random value of $C_{d_1,r}(k)$. Because D_1 no longer impose buffering on the arrival data, we are able to impose the strictest QoS constraints at R, and assume that $\bar{\theta}$ is unbounded. It means that any value of $\hat{\theta} \leq \bar{\theta}$. With these assumptions, we can say that $r_a = EC_R(\hat{\theta})$ and $EC_R(\hat{\theta}) \leq EC_R(\theta_r)$ where $\hat{\theta} \geq \theta_r$. We also observe that $EC_R(\hat{\theta})$ is a monotonically decreasing function of $\hat{\theta}$. From here, we can see that the maximum value r_a can get is $EC_R(\theta_r)$ when there is no buffer constraints imposed at D_1. By combining both of these bounds, we can conclude that r_a is bounded by the minimum of the EC at D_1 and R.

5 | NUMERICAL RESULTS

5.1 | Simulation setup

We consider a cell of radius 500 m and randomly place source, destination, and relay nodes. For the proposed multiple features-based mode selection method, we consider the following (slowly-varying) features: distance, path loss, and RSSI. To this end, we use the following path loss model: $PL(d) = 128.1 + 37.6 \log_{10}(d)$ and the Friss transmission formula for RSSI. We use antenna gain of 1 dB at the transmitter, receiver, and relay antennas. We consider a channel bandwidth of

10 kHz. We also assume that the prior probabilities of selecting a communication mode are equal to each other; therefore, both the error probabilities are equal to each other ($P_{e,1} = P_{e,2}$). We also assume that the channels $D_1 \rightarrow D_2$, $D_1 \rightarrow R$, and $R \rightarrow D_2$ follows independent Rayleigh fading.

5.2 | Simulation results

Figure 5 presents the error and correct detection probabilities for different values of the standard deviation of the features' estimation error (σ_T). The error probability increases with increasing estimation error; the correct detection decreases with increasing estimation error. This rate of increase can be limited by using the optimal weights for the underlying features. It is evident from Figure 5 that the error probability with optimal features' weights is much less than that with heuristically assigned weights. It shows the efficacy of Algorithm 1 for generating optimal weights for the underlying features. Moreover, we have compared our results with the model proposed in Reference 16, which uses path loss as the sole feature for mode selection. We show that mode selection based on multiple features performs better than mode selection based on a single feature (path loss[16]) only, when optimal weights are assigned to the underlying features.

Similarly, Figure 6 shows the KLD and error probabilities compared to the standard deviation of the estimation error (σ_T) for a different set of features' weights. KLD decreases exponentially fast with an increase in estimation error and reaches zero for $\sigma_T < 6$. However, the KLD with optimal weights is much greater than the KLD with heuristically assigned weights when $\sigma_T < 1$. The KLD with optimal weights reaches zero at $\sigma_T = 10$, whereas, the KLD with heuristically assigned weights reaches zero at $\sigma_T = 5$. It shows that with efficient estimators (or with a joint estimator) for underlying features, KLD with optimal weights will provide much better (at least 2.5×) results as compared to KLD with heuristically assigned features' weights. Moreover, we have also compared our results with KLD of the model proposed in Reference 16. Our model provides KLD of 790 at $\sigma_T = 0.4$, whereas, the model in Reference 16 provides KLD of 450 for the same σ_T, which shows the better performance of our model.

Figure 7 presents the EC for different values of $\gamma_r(k)$. The EC increases with an increase of $\gamma_r(k)$. However, statistical bounds on the transmitter's queue (Q_d) limit this increase. It is because the EC is a function of SNR as well as delay bounds on the transmitter's queue, unlike Shannon's capacity, which is only the function of SNR. We observe that as θ_d increases, the increase in the EC is bounded. For $\theta_d = 0.2$, the EC increases exponentially fast for $\gamma_r(k) \leq 19$. Soon after that, it retains its maximum value of 288 bits/second (bps). On the other hand, for $\theta_d = 0.8$, the EC jumps from 68 to 72 bps as $\gamma_r(k)$ increases from 1 to 2 dB. After that, it retains this value as $\gamma_r(k)$ increases. It is due to the fact that if strict QoS constraints are imposed at the transmitter's queue, then SNR or the channel conditions will not be the limiting factor for the EC.
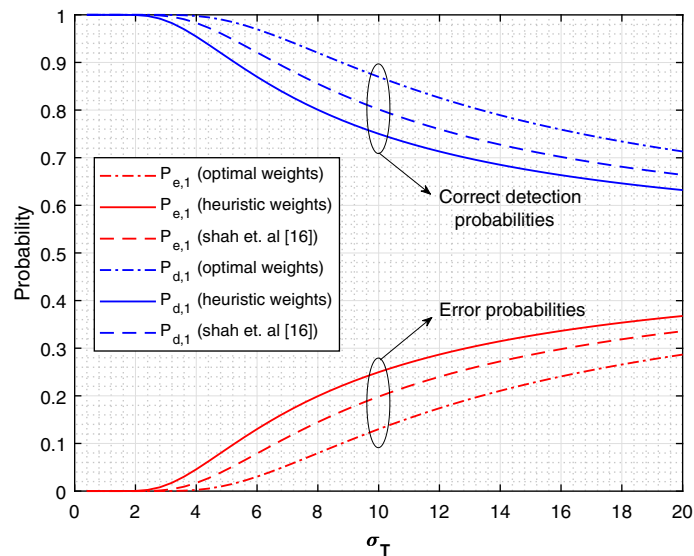

FIGURE 5 Correct detection and error probabilities vs standard deviation of the estimation error (σ_T) for different set of weights. Feature weights are assigned in two different ways; optimal (according to Algorithm 1) and heuristic ($w_i = 1/\sigma_i$)
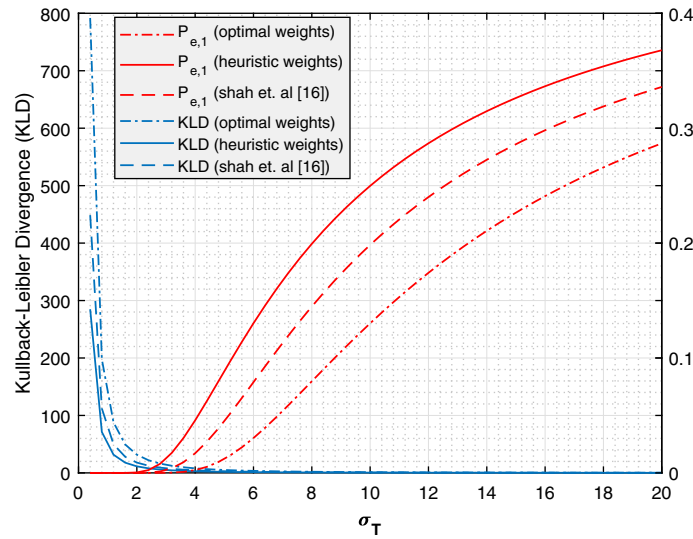
FIGURE 6 KLD and error probability ($P_{e,1}$) vs standard deviation of the estimation error (σ_T) for different set of weights
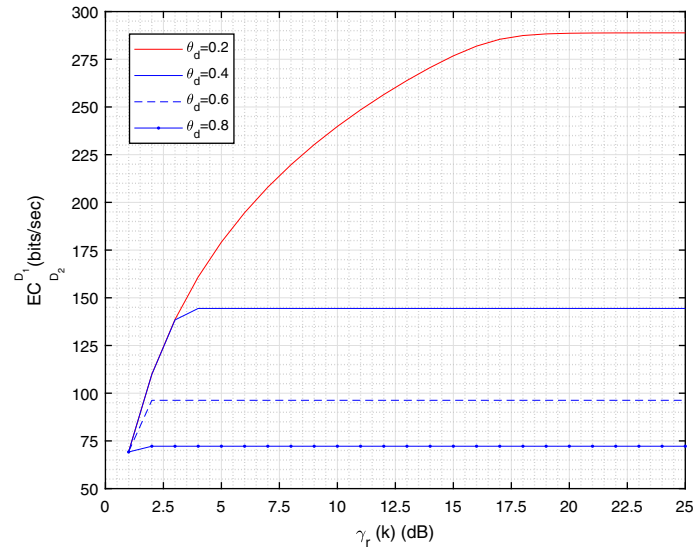

FIGURE 7 $EC_{D_2}^{D_1}(\theta_d, \theta_r)$ vs SINR ($\gamma_r(k)$) for different QoS exponent (θ_d)

Figure 8 presents EC_{D_1} for different QoS constraints θ_d. EC_{D_1} decreases exponentially fast with an increase in θ_d for the range of $0.1 < \theta_d < 0.3$. This decreasing trend remains intact for $\theta_d > 0.3$; however, the rate of decrease reduced. Additionally, we also investigate the impact of using optimal transmission power on the EC of relay-D2D link. We observe that better EC can be achieved with optimal transmission power strategy as compared to maximum transmission power. It is because using maximum transmission power at the relay node leads to an increase in interference as well as SI. The gain of using optimal transmit powers over maximum transmit powers diminishes as more strict QoS constraints imposed at the transmitter's queue. Further, we can see that, when keeping the relay transmission power the same (using optimal transmit power), the power class-1 device (33 dBm transmission power) provides better EC compared to the power class-2 device (27 dBm transmission power). This phenomenon is inline with the optimization problem for $P_{d_1}^{opt}$ in Equation (27), which states that maximum transmit power is the optimal transmit power at the transmitter ($P_{d_1}^{opt} = P_{d_1}^{max}$).

Figure 9 presents EC_{D_1} with varying quality of analog and digital SI cancellation techniques (β). Note that we are using residual SI as a factor of noise in our analysis. The better the quality of the employed SI cancellation techniques, the less the residual SI, and in turn, the better the EC_{D_1}. It is evident from Figure 9 that EC_{D_1} increases with an increase in β, and reaches
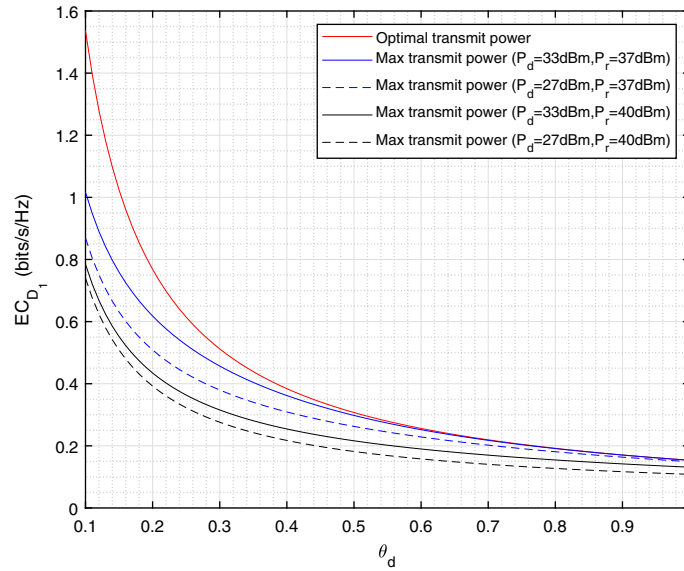
FIGURE 8 Effective capacity (EC_{D_1}) vs QoS exponent (θ_d) for optimal and maximum power transmissions
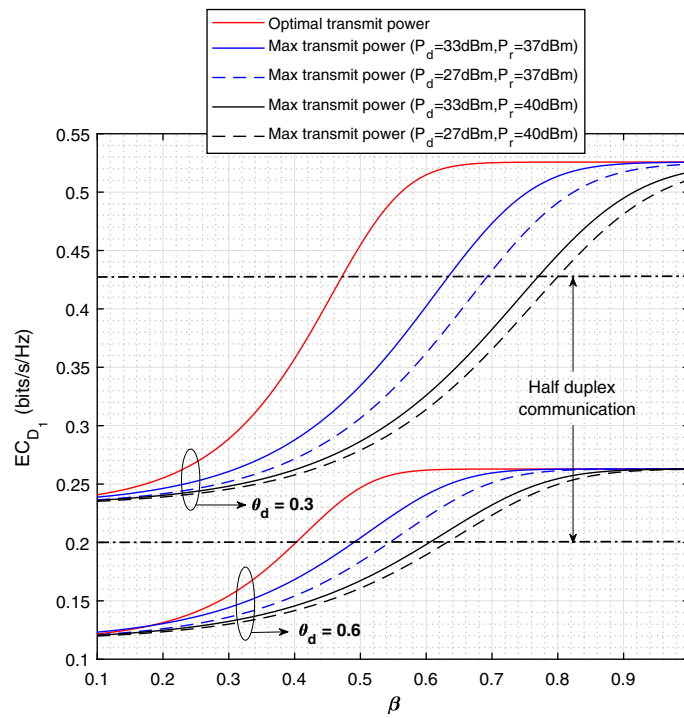

FIGURE 9 Effective capacity (EC_{D_1}) vs quality of SI cancellation techniques (β) for optimal and maximum power transmissions

to the maximum when β approaches 1, which means perfect SI cancellation. Additionally, the efficacy of the transmit power optimization can also be seen in that the maximum EC_{D_1} is attained when $\beta = 0.68$ for $\theta_d = 0.3$ and $\beta = 0.58$ for $\theta_d = 0.6$. Contrarily, when no transmit power optimization is used, then the same EC_{D_1} is attained when $\beta > 0.92$ for $\theta_d = 0.3$ and $\beta > 0.74$ for $\theta_d = 0.6$. It shows the efficacy of using the proposed optimization problem for optimal transmit power. Further, we observe the impact of using different power class devices (at D_1 and R) on SI cancellation as well as on the EC. One can see that as we increase the power class of the transmitting device, the EC increases. Whereas, the EC decreases with an increase in the power class of the relay device. It is because high power class device at the relay node causes more SI. Lastly, the impact of β on half-duplex communication is also presented for a fair comparison with FD communication. We observe that our proposed system of D2D communication with an FD relay can achieve similar EC
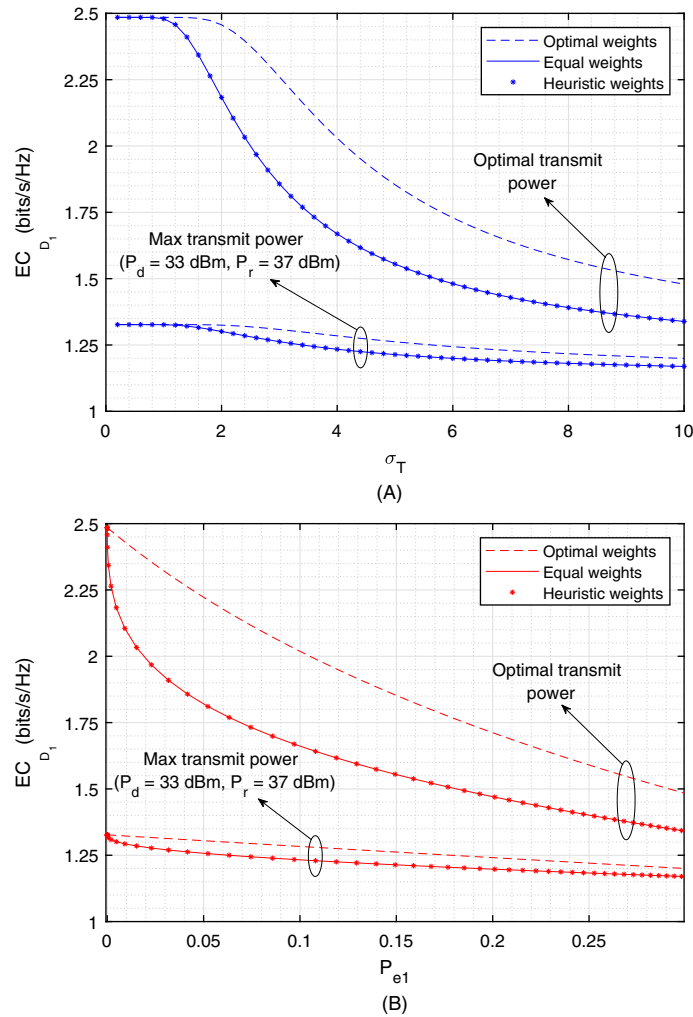
FIGURE 10 Impact of mode selection on the EC, A, EC_{D_1} vs σ_T for different set of weights, B, EC_{D_1} vs $P_{e,1}$ for different set of weights

as of half-duplex relay using optimal transmission powers when the quality of SI cancellation techniques reaches 0.48 (for $\theta = 0.3$) and 0.40 (for $\theta = 0.6$).

Figure 10 presents the impact of mode selection on EC_{D_1}. Figure 10A shows that EC_{D_1} decreases with an increase in σ_T. The rate of decrease of EC_{D_1} when D_1 and R are transmitting with optimal powers is much higher than that when maximum transmit power is used. However, EC_{D_1} with optimal transmit power remains significantly higher than its counterpart even for higher values of σ_T. One can see a similar result in Figure 10B, where EC_{D_1} is presented for different values of $P_{e,1}$. This figure demonstrates that to get maximum benefits of transmit power optimization, efficient estimators are required for wireless channel features. Last but not least, Figure 10A,B both show the effect of weight optimization on EC_{D_1} versus σ_T and $P_{e,1}$.

6 | CONCLUSION

We considered a spectrum sharing D2D network in which a transmitting device communicates with its receiver through an FD relay under the delay QoS constraints required for successful transmission. We provided the EC analysis of the relay-assisted D2D communication. We identified the effects of having delay QoS constraints at both the transmitter and the relay node upon the EC of the relay-D2D link. We incorporated the residual SI caused by the FD relaying as a factor of noise in our analysis. We noted that the SI cancellation techniques employed at the relay node have a direct impact on the EC of relay-D2D link, and the EC increases with an increase in the quality of SI cancellation techniques. Using optimal transmit power, the EC of FD communication can reach the EC of half-duplex communication when the quality of SI

cancellation techniques is 0.6. We also noted that when strict QoS constraints are imposed, increasing SINR does not affect the EC of relay-assisted D2D communication. We found that a better EC can be achieved by using optimal transmit power and optimal weights (for the features utilized by the mode selection). When $P_{e,1} = 0.01$, EC of 2.45 bits/s/Hz is achieved with optimal transmit power and optimal weights, whereas slightly more than half of it (1.3 bits/s/Hz) is achieved by using maximum transmit power and heuristic weights. Additionally, we observed that maximum EC can be achieved when the standard deviation of the estimation error is less than 2 ($\sigma_T < 2$); therefore, designing efficient estimators meeting the Cramer Rao Bound is of paramount importance.

DATA AVAILABILITY STATEMENT
We do not have any data to share.

ORCID
Syed Waqas Haider Shah https://orcid.org/0000-0001-5108-3705

Muhammad Mahboob Ur Rahman https://orcid.org/0000-0002-6768-0886

Waqas Aman https://orcid.org/0000-0002-2443-1302

Jon Crowcroft https://orcid.org/0000-0002-7013-0121

REFERENCES
1. Bahonar MH, Omidi MJ. Distributed pricing-based resource allocation for dense device-to-device communications in beyond 5g networks. *Trans Emerg Telecommun Technol*. 2021;e4250.
2. Hasan M, Hossain E, Kim DI. Resource allocation under channel uncertainties for relay-aided device-to-device communication underlaying LTE-A cellular networks. *IEEE Trans Wirel Commun*. 2014;13(4):2322-2338.
3. Viswanathan H, Mukherjee S. Performance of cellular networks with relays and centralized scheduling. *IEEE Trans Wirel Commun*. 2005;4(5):2318-2328.
4. Shin W, Yang H, Vaezi M, Lee J, Poor HV. Relay-aided NOMA in uplink cellular networks. *IEEE Signal Process Lett*. 2017;24(12):1842-1846.
5. Lu W, Di Renzo M. Stochastic geometry modeling and system-level analysis & optimization of relay-aided downlink cellular networks. *IEEE Trans Commun*. 2015;63(11):4063-4085.
6. Baştürk İ, Chen Y, Alouini M-S. Energy-efficient communication for user-relay aided cellular networks with OFDMA. *Phys Commun*. 2019;33:153-164.
7. Madani Fadoul M, Nour Hindia M, Dimyati K, Hanafi E, Sadegh Amiri I. Oblique projection: an interference mitigation for MIMO multihop full-duplex relay. *Trans Emerg Telecommun Technol*. 2020;31(4):e3799.
8. Ma R, Chang Y-J, Chen H-H, Chiu C-Y. On relay selection schemes for relay-assisted D2D communications in LTE-A systems. *IEEE Trans Veh Technol*. 2017;66(9):8303-8314.
9. Zhang Z, Zhang P, Liu D, Sun S. SRSM-based adaptive relay selection for D2D communications. *IEEE Internet Things J*. 2017;5(4):2323-2332.
10. Li Y, Zhang Z, Wang H, Yang Q. SERS: social-aware energy-efficient relay selection in D2D communications. *IEEE Trans Veh Technol*. 2018;67(6):5331-5345.
11. Ma R, Xia N, Chen H-H, Chiu C-Y, Yang C-S. Mode selection, radio resource allocation, and power coordination in d2d communications. *IEEE Wirel Commun*. 2017;24(3):112-121.
12. Dang S, Coon JP, Chen G. Resource allocation for full-duplex relay-assisted device-to-device multicarrier systems. *IEEE Wirel Commun Lett*. 2017;6(2):166-169.
13. Wang K, Heng W, Li X, Wu J, Hu J, Wang G. Energy-efficient resource allocation for full-duplex relay-assisted D2D communications. Paper presented at: Proceedings of the IEEE Wireless Communications and Networking Conference (WCNC), Marrakesh, Morocco; 2019:1-6.
14. Yang Y, Zhang Y, Dai L, Li J, Mumtaz S, Rodriguez J. Transmission capacity analysis of relay-assisted device-to-device overlay/underlay communication. *IEEE Trans Ind Inform*. 2017;13(1):380-389.
15. Amodu OA, Othman M, Noordin NK, Ahmad I. Transmission capacity analysis of relay-assisted D2D cellular networks with M2M coexistence. *Comput Netw*. 2019;164:106887.
16. Shah SWH, Rahman MMU, Mian AN, Imran A, Mumtaz S, Dobre OA. On the impact of mode selection on effective capacity of device-to-device communication. *IEEE Wirel Commun Lett*. 2019;8(3):945-948.
17. Ismaiel B, Abolhasan M, Ni W, Smith D, Franklin D, Jamalipour A. Analysis of effective capacity and throughput of polling-based device-to-device networks. *IEEE Trans Veh Technol*. 2018;67(9):8656-8666.
18. Chang C-S. Stability, queue length, and delay of deterministic and stochastic queueing networks. *IEEE Trans Automat Contr*. 1994;39(5):913-931.
19. Wu D, Negi R. Effective capacity: a wireless link model for support of quality of service. *IEEE Trans Wirel Commun*. 2003;2(4):630-643.
20. Akin S, Gursoy MC. Effective capacity analysis of cognitive radio channels for quality of service provisioning. *IEEE Trans Wirel Commun*. 2010;9(11):3354-3364.

21. Gamage S, Ngo DT, Khan JY. Statistical delay-qos driven resource allocation for multiuser cognitive radio networks. Paper presented at: Proceedings of the IEEE Wireless Communications and Networking Conference (WCNC), Barcelona, Spain; 2018:1-6

22. Abdel-Malek MA, Seddik KG, ElBatt T, Mohasseb Y. Effective capacity optimization for cognitive radio networks under primary QoS provisioning. *Wirel Netw*. 2020;26(3):2171-2190.

23. Xiao C, Zeng J, Ni W, Liu RP, Su X, Wang J. Delay guarantee and effective capacity of downlink NOMA fading channels. *IEEE J Select Top Signal Process*. 2019;13(3):508-523.

24. Yu W, Chorti A, Musavian L, Poor HV, Ni Q. Effective secrecy rate for a downlink NOMA network. *IEEE Trans Wirel Commun*. 2019;18(12):5673-5690.

25. Zhang X, Wang J, Poor HV. NOMA-based statistical QoS provisioning for wireless ad-hoc networks with finite blocklength. Paper presented at: Proceedings of the IEEE Global Communications Conference (GLOBECOM), Waikoloa, HI, USA; 2019:1-6.

26. Qiao D, Gursoy MC, Velipasalar S. Effective capacity of two-hop wireless communication systems. *IEEE Trans Inf Theory*. 2013;59(2):873-885.

27. Li J, Ding Y, Ye Q, Zhang N, Zhuang W. On effective capacity and effective energy efficiency in relay-assisted wireless networks. *IEEE Trans Veh Technol*. 2017;67(5):4389-4400.

28. Qiao D. Outage effective capacity of buffer-aided diamond relay systems using HARQ-IR. *IEEE Trans Veh Technol*. 2018;68(1):540-553.

29. Aman W, Haider Z, Shah SWH, Rahman M, Dobre OA. On the effective capacity of an underwater acoustic channel under impersonation attack; 2020. arXiv preprint arXiv:2002.05093.

30. Shah SWH, Mian AN, Crowcroft J. Statistical QoS guarantees for licensed-unlicensed spectrum interoperable D2D communication. *IEEE Access*. 2020;8:27 277-27 290.

31. Amjad M, Musavian L, Rehmani MH. Effective capacity in wireless networks: a comprehensive survey. *IEEE Commun Surv Tutor*. 2019;21(4):3007-3038.

32. Doppler K, Yu CH, Ribeiro CB, Janis P. Mode selection for device-to-device communication underlaying an lte-advanced network. Paper presented at: Proceedings of the IEEE Wireless Communication and Networking Conference (WCNC), Sydney, NSW, Australia; 2010:1-6.

33. Gross J Scheduling with outdated CSI: effective service capacities of optimistic vs. pessimistic policies. Paper presented at: Proceedings of the IEEE 20th International Workshop on Quality of Service, Coimbra, Portugal; 2012:1-9.

34. Jain M, Choi JI, Kim T, et al. Practical, real-time, full duplex wireless. Paper presented at: Proceedings of the ACM 17th Annual International Conference on Mobile Computing and Networking, Las Vegas Nevada USA; 2011:301-312.

35. Choi JI, Jain M, Srinivasan K, Levis P, Katti S. Achieving single channel, full duplex wireless communication. Paper presented at: Proceedings of the ACM 16th Annual International Conference on Mobile Computing and Networking, Chicago Illinois USA; 2010:1-12.

36. Omri A, Hasna MO. A distance-based mode selection scheme for D2D-enabled networks with mobility. *IEEE Trans Wirel Commun*. 2018;17(7):4326-4340.

37. Mahmood K, Kurt GK, Ali I. Mode selection rules for device-to-device communication: design criteria and performance metrics. Paper presented at: Proceedings of the IEEE International Symposium on Signal Processing and Information Technology, Athens, Greece: IEEE; 2013:000 315-000 320.

38. Hong M, Sun R, Baligh H, Luo Z-Q. Joint base station clustering and beamformer design for partial coordinated transmission in heterogeneous networks. *IEEE J Select Areas Commun*. 2013;31(2):226-240.

39. Chang C-S, Zajic T. Effective bandwidths of departure processes from queues with time varying capacities. *Proceedings of IEEE INFOCOM*. Vol 3; IEEE; 1995:1001-1009.

40. Duarte M, Dick C, Sabharwal A. Experiment-driven characterization of full-duplex wireless systems. *IEEE Trans Wirel Commun*. 2012;11(12):4296-4307.

41. Wang Y, Yin W, Zeng J. Global convergence of admm in nonconvex nonsmooth optimization. *J Sci Comput*. 2019;78(1):29-63.

42. Chang C-S. *Performance Guarantees in Communication Networks*. Berlin, Germany: Springer Science & Business Media; 2012.

APPENDIX A. A PROOF OF LEMMA 1

For an equation $y = \mathbf{x}^T \mathbf{A} \mathbf{x}$, where $\mathbf{x}$ and $\mathbf{A}$ are $N \times 1$ vector and symmetric matrix of the order $N \times N$, respectively, we have

$$\frac{\partial y}{\partial \mathbf{x}} = 2\mathbf{x}^T \mathbf{A} \tag{A1}$$

and

$$dA^{-1} = -A^{-1}dAA^{-1} \tag{A2}$$

For an equation $f = \frac{X}{Y} = \frac{\mathbf{x}^T \mathbf{A} \mathbf{x}}{\mathbf{x}^T \mathbf{B} \mathbf{x}}$, where X and Y are the functions of x, and $\mathbf{B}$ is a symmetric matrix of the order $N \times N$. We have

$$
\begin{aligned}
df &= \operatorname{tr}\{dX \cdot Y^{-1} + X \cdot d(Y^{-1})\} \\
&= \operatorname{tr}\{dX \cdot Y^{-1} + X \cdot (-Y^{-1}dYY^{-1})\} \\
&= \operatorname{tr}\left\{ \frac{2\mathbf{x}^T \mathbf{A} d\mathbf{x}}{\mathbf{x}^T \mathbf{B} \mathbf{x}} - \frac{\mathbf{x}^T \mathbf{A} \mathbf{x} 2 \mathbf{x}^T B d\mathbf{x}}{(\mathbf{x}^T \mathbf{B} \mathbf{x})^2} \right\} \\
&= \frac{\mathbf{x}^T \mathbf{B} \mathbf{x} 2 \mathbf{x}^T \mathbf{A} d\mathbf{x} - \mathbf{x}^T \mathbf{A} \mathbf{x} 2 \mathbf{x}^T \mathbf{B} d\mathbf{x}}{(\mathbf{x}^T \mathbf{B} \mathbf{x})^2}
\end{aligned}
\tag{A3}
$$

Therefore,

$$\frac{\partial f}{\partial \mathbf{x}} = 2 \frac{\mathbf{x}^T \mathbf{B} \mathbf{x} \mathbf{x}^T A - \mathbf{x}^T \mathbf{A} \mathbf{x} \mathbf{x}^T B}{(\mathbf{x}^T \mathbf{B} \mathbf{x})^2} \tag{A4}$$

If A is a positive, semidefinite matrix like Ω_m and B is a positive matrix like Λ_{σ^2}, $\frac{\partial f}{\partial \mathbf{x}}$ is neither always positive nor negative. The lemma holds.

APPENDIX B. B PROOF OF LEMMA 2

Considering the $|\mathbf{w}| = 1$ constraint, the upper bound likely becomes a homogeneous quadratic function that takes the form $\mathbf{w}^T \mathbf{C} \mathbf{w}$, which can be conveniently solved as an eigenvalue problem. The remaining difficulty lies in the term $\left\| \Omega_m^{\frac{1}{2}} \mathbf{w} \right\| \left\| \Lambda_{\sigma^2}^{\frac{1}{2}} \mathbf{w} \right\|$.

Taking account of the Cauchy-Schwartz inequality, for any vectors $\mathbf{x}, \mathbf{y}, \tilde{\mathbf{x}} \neq 0$ and $\tilde{\mathbf{y}} \neq 0$ we have

$$\|\mathbf{x}\| \|\mathbf{y}\| \geq \frac{1}{\|\tilde{\mathbf{x}}\| \|\tilde{\mathbf{y}}\|} \mathbf{x}^T \tilde{\mathbf{x}} \tilde{\mathbf{y}}^T \mathbf{y} \tag{B1}$$

$$
\begin{aligned}
\min_{\{w_i\}_{i=1}^N} v(\mathbf{w}) &\leq \min_{\{w_i\}_{i=1}^N} \tilde{v}(\mathbf{w}; \tilde{\mathbf{w}}) = \min_{\{w_i\}_{i=1}^N} \mathbf{w}^T \Omega_m \mathbf{w} + t^2 \mathbf{w} \Lambda_{\sigma^2} \mathbf{w} - t\mathbf{w}^T \frac{\Lambda_{\sigma^2} \tilde{\mathbf{w}} \tilde{\mathbf{w}}^T \Omega_m + \Omega_m \tilde{\mathbf{w}} \tilde{\mathbf{w}}^T \Lambda_{\sigma^2}}{\left\| \Omega_m^{\frac{1}{2}} \tilde{\mathbf{w}} \right\| \left\| \Lambda_{\sigma^2}^{\frac{1}{2}} \tilde{\mathbf{w}} \right\|} \mathbf{w} \\
&= \min_{\{w_i\}_{i=1}^N} \mathbf{w}^T \left\{ \Omega_m + t^2 \Lambda_{\sigma^2} - t \frac{\Lambda_{\sigma^2} \tilde{\mathbf{w}} \tilde{\mathbf{w}}^T \Omega_m + \Omega_m \tilde{\mathbf{w}} \tilde{\mathbf{w}}^T \Lambda_{\sigma^2}}{\left\| \Omega_m^{\frac{1}{2}} \tilde{\mathbf{w}} \right\| \left\| \Lambda_{\sigma^2}^{\frac{1}{2}} \tilde{\mathbf{w}} \right\|} \right\} \mathbf{w}
\end{aligned}
$$

$$\text{Subject to: } |\mathbf{w}| = \sum_{i=1}^N w_i = 1 \tag{B2}$$

Hence, we denote $\tilde{\mathbf{w}}$ as an approximation of $\mathbf{w}$ at a previous iteration. The optimization problem in (14) could be re-formulated as (B2).

Therefore, the optimization problem in (B2) could be rewritten as a Lagrangian format, namely (15), where λ_w denotes a Lagrangian factor.

APPENDIX C. C PROOF OF CONVERGENCE OF ALGORITHM 1

For an optimization problem that is possibly non-smooth and non-convex,

$$\min_{\mathbf{x}_0, \mathbf{x}_1, \ldots, \mathbf{x}_p, y} \phi(\mathbf{x}_0, \mathbf{x}_1, \ldots, \mathbf{x}_p, y)$$

$$\text{s.t.: } \mathbf{A}_0 \mathbf{x}_0 + \mathbf{A}_1 \mathbf{x}_1 + \ldots + \mathbf{A}_p \mathbf{x}_p + \mathbf{B} y = b \tag{C1}$$

where $\phi : \mathbb{R}^{n_0} \times \dots \times \mathbb{R}^{n_p} \times \mathbb{R}^q \to \mathbb{R} \cup \{\infty\}$ is a continuous function. $x_i \in \mathbb{R}^{n_i}$ are the variables. $\mathbf{A}_i \in \mathbb{R}^{m \times n_i}$ are the coefficient matrices of these variables, where $i = 0, \dots, p, y \in \mathbb{R}^q$. The coefficient matrix of the last variable $y \in \mathbb{R}^q$ is $\mathbf{B} \in \mathbb{R}^{m \times q}$.

Lemma 5 (Theorem 1 of[41]). *For problem defined in (C1), if the followings conditions hold,*

1) *(Feasibility)* $\mathrm{Im}(\mathbf{A}) \subseteq \mathrm{Im}(\mathbf{B})$*, where* $\mathrm{Im}(\cdot)$ *denotes the image of a matrix.*
2) *(Coercivity) Let* $\mathcal{F} := (\mathbf{x}, \mathbf{y})$ *be a feasible set, where* $(\mathbf{x}, \mathbf{y}) \in \mathbb{R}^{n+q}$ *and* $\mathbf{Ax} + \mathbf{By} = \mathbf{0}$*. Then the objective function* $\phi(\mathbf{x}, \mathbf{y})$ *is coercive over the feasible set* $\mathcal{F}$*, meaning that* $\phi(\mathbf{x}, \mathbf{y})$ *approaches* ∞ *if* $(\mathbf{x}, \mathbf{y}) \in \mathcal{F}$ *and* $\|(\mathbf{x}, \mathbf{y})\|$ *approaches* ∞*.*
3) *(Lipschitz sub-minimization paths)*
   - *For any fixed* $\mathbf{x}$*,* $\arg\min_\mathbf{y}\{\phi(\mathbf{x}, \mathbf{y}) : \mathbf{By} = \mathbf{u}\}$ *has a unique minimizer.* $H(\mathbf{u}) := \arg\min\{\phi(\mathbf{x}, \mathbf{y}) : \mathbf{By} = \mathbf{u}\}$ *defines* $H : \mathrm{Im}(B) \to \mathbb{R}^q$*, which is a Lipschitz continuous map.*
   - *For* $i = 0, \dots, p$ *and any* $\mathbf{x}_{<i}$*,* $\mathbf{x}_{>i}$ *and* $\mathbf{y}$*,* $\arg\min_{\mathbf{x}_i}\{\phi(\mathbf{x}_{<i}, \mathbf{x}_i, \mathbf{x}_{>i}, \mathbf{y}) : \mathbf{A}_i\mathbf{x}_i = \mathbf{u}\}$ *has a unique minimizer and* $F_i :$ $\mathrm{Im}(\mathbf{A}_i) \to \mathbb{R}^{n_i}$ *defined by* $F_i(\mathbf{u}) := \arg\min_{\mathbf{x}_i}\{\phi(\mathbf{x}_{<i}, \mathbf{x}_i, \mathbf{x}_{>i}, \mathbf{y}) : \mathbf{A}_i\mathbf{x}_i = \mathbf{u}\}$ *is a Lipschitz continuous map.*
4) *(Objective-f regularity) f has the form*

$$f(\mathbf{x}) := g(\mathbf{x}) + \sum_{i=0}^{p} f_i((x)_i) \tag{C2}$$

   where
   - $g(\mathbf{x})$ *is a Lipschitz differentiable and has a constant* L_g*,*
   - *Either*

     – f_0 *is a lower semi-continuous function, and* $f_i((x)_i)$ *is a restricted prox-regular function[41] for* $i = 1, \dots, p$*.*
     – *The supremum* $\sup\{\|d\| : \mathbf{x}_0 \in S, d \in \partial f_0(\mathbf{x}_0)\}$ *is bounded for any bounded set S,* $f_i(\mathbf{x}_i)$ *is continuous and piecewise linear[41] for* $i = 1, \dots, p$*.*

5) *(Objective-h regularity)* $h(\mathbf{y})$ *is Lipschitz differentiable with constant* L_h*.*

   then we have the ADMM algorithm converges subsequently.

Proof. We notice that the problem defined in (11) is a special case of[41] with $p = 0$, $\mathbf{A}_0 = [1, \dots, 1]$, $\mathbf{y} = 0$ and $b = 1$.

In particular, t and $\mathbf{w}$ are bounded and for each sub-problem, it has one unique maximizer. Hence, the conditions (1), (2), and (3) hold. Meanwhile, for any sequence $\mathbf{w}_1$, $\mathbf{w}_2$, and matrix $\mathbf{A}$, since

$$\left| \|\Omega_m^{1/2}\mathbf{w}_1\| - \|\Omega_m^{1/2}\mathbf{w}_2\| \right| \overset{(a)}{\le} \|\Omega_m^{1/2}(\mathbf{w}_1 - \mathbf{w}_2)\|$$
$$= \sqrt{(\mathbf{w}_1 - \mathbf{w}_2)^T \Omega_m (\mathbf{w}_1 - \mathbf{w}_2)}$$

where the inequality (a) comes from the triangular inequality, there exists a constant K satisfying $\left| \|\Omega_m^{1/2}\mathbf{w}_1\| - \|\Omega_m^{1/2}\mathbf{w}_2\| \right| \le K(\mathbf{w}_1 - \mathbf{w}_2)$. In other words, $\|\Omega_m^{1/2}\mathbf{w}\|$ is Lipschitz continuous. Also, the first derivative $\|\Omega_m^{1/2}\mathbf{w}\|$ is bounded for $w_i > 0, \forall i \in (1, \dots, N)$. Hence, $\|\Omega_m^{1/2}\mathbf{w}\|$ is Lipschitz differentiable in the field of $w_i > 0, \forall i \in (1, \dots, N)$. Similarly, $\|\Lambda_m^{1/2}\mathbf{w}\|$ is Lipschitz differentiable in the field of $w_i > 0, \forall i \in (1, \dots, N)$. Therefore, the condition 4) holds.

Based on the analyses of Reference 41, given all conditions in Lemma 5, the convergence of Algorithm 1 has been established. ∎

APPENDIX D. D PROOF OF LEMMA 3

In our case, the D2D channel is a Markov service process. Therefore, the service process rate at D_1 can be regarded as a Markov modulated process, and then the EC at D_1 can be written as:[42]

$$EC_{D_1} = -\frac{\Lambda(-\theta_d)}{\theta_d} = -\frac{1}{\theta_d} \log_e \mathrm{sp}(\boldsymbol{\Phi_1}(-\theta_d)\mathbf{P}). \tag{D1}$$

It shows that log-MGF for $S_1(t)$ can be represented as $\mathrm{sp}(\boldsymbol{\Phi_1}(-\theta_d)\mathbf{P})$. Where $\mathrm{sp}(.)$ is the spectral radius. To find $\mathrm{sp}(\boldsymbol{\Phi_1}(-\theta_d)\mathbf{P})$, $\mathbf{P}$ is a matrix containing state transition probabilities at D_1 given in (32) and $\boldsymbol{\Phi_1}(-\theta_d)$ can be found by finding the log-MGF for the states at D_1. From Table 2, we know that $S_1(k) = r_d(k)$ in states s_1 and s_3, $S_1(k) = r_r(k)$ in state S_4, and $S_1(k) = 0$ in state S_2. Therefore, the log-MGFs would be $\phi_1(\theta_d) = \phi_3(\theta_d) = \mathbb{E}_{z_1}[e^{r_d(k)\theta_d}]$, $\phi_4(\theta_d) = \mathbb{E}_{z_{r1}}[e^{r_r(k)\theta_d}]$, and $\phi_2(\theta_d) = 0$, where $\mathbb{E}_{z_1}$ and $\mathbb{E}_{z_{r1}}$ are the expectation with respect to the $D_1 \rightarrow D_2$ and $D_1 \rightarrow R$ link conditions, respectively. Thus, $\boldsymbol{\Phi_1}(\theta_d)$ is as follows:

$$\boldsymbol{\Phi_1}(\theta_d) = \mathrm{diag}\left(\mathbb{E}_{z_1}[e^{r_d(k)\theta_d}], 1, \mathbb{E}_{z_1}[e^{r_d(k)\theta_d}], \mathbb{E}_{z_{r1}}[e^{r_r(k)\theta_d}]\right) \tag{D2}$$

Because $\boldsymbol{\Phi_1}(\theta_d)\mathbf{P}$ is a unit-rank matrix, one can determine its spectral radius by finding its trace:

$$\begin{aligned} \mathrm{sp}(\boldsymbol{\Phi_1}(\theta_d)\mathbf{P}) &= \mathrm{trace}[\boldsymbol{\Phi_1}(\theta_d)\mathbf{P}] \\ &= p_1\mathbb{E}_{z_1}[e^{r_d(k)\theta_d}] + p_2 + p_3\mathbb{E}_{z_1}[e^{r_d(k)\theta_d}] + p_4\mathbb{E}_{z_{r1}}[e^{r_r(k)\theta_d}] \end{aligned} \tag{D3}$$

By substituting (D3) in (D1), the EC at D_1 can be written as,

$$EC_{D_1} = -\frac{1}{\theta_d}\log_e\left((p_1 + p_3)\mathbb{E}_{z_1}[e^{-r_d(k)\theta_d}] + p_2 + p_4\mathbb{E}_{z_{r1}}[e^{-r_r(k)\theta_d}]\right) \tag{D4}$$

APPENDIX E. PROOF OF LEMMA 4

Similar to Lemma 3, the EC at R can be written as

$$EC_R = -\frac{\Lambda(-\theta_r)}{\theta_r} = -\frac{1}{\theta_r}\log_e \mathrm{sp}(\boldsymbol{\Phi_2}(-\theta_r)\mathbf{Q}) \tag{E1}$$

where $\boldsymbol{\Phi_2}(\theta_r)$ can be found by finding the log-MGFs of the processes in the two states at R. We know that $S_2(k) = 0$ for state m_1 and $S_2(k) = C_{r,d_2}(k)$ for state m_2. Therefore, the corresponding MGFs of the two states are $\phi_1(\theta_r) = \mathbb{E}_{z_{r2}}[e^{C_{r,d_2}(k)\theta_r}]$ and $\phi_2(\theta_r) = 1$, where $\mathbb{E}_{z_{r2}}$ is the expectation with respect to the $R \rightarrow D_2$ link conditions. Thus, $\boldsymbol{\Phi_2}(\theta_r)$ is as follows:

$$\boldsymbol{\Phi_2}(\theta_r) = \mathrm{diag}(\mathbb{E}_{z_{r2}}[e^{C_{r,d_2}(k)\theta_r}], 1) \tag{E2}$$

Then we can write

$$\boldsymbol{\Phi_2}(\theta_r)\mathbf{R} = \begin{bmatrix} \phi_1(\theta_r)R_1 & \phi_1(\theta_r)R_2 \\ \phi_2(\theta_r)R_1 & \phi_2(\theta_r)R_2 \end{bmatrix} \tag{E3}$$

because $\boldsymbol{\Phi_2}(\theta_r)\mathbf{R}$ is a unit-rank matrix. Therefore, finding $\mathrm{sp}(\boldsymbol{\Phi_2}(\theta_r)\mathbf{R})$ is equivalent to finding $\mathrm{trace}(\boldsymbol{\Phi_2}(\theta_r)\mathbf{R})$:

$$\begin{aligned} \mathrm{sp}(\boldsymbol{\Phi_2}(\theta_r)\mathbf{R}) &= \mathrm{trace}[\boldsymbol{\Phi_2}(\theta_r)\mathbf{R}] \\ &= R_1\mathbb{E}_{z_{r2}}[e^{C_{r,d_2}(k)\theta_r}] + R_2 \end{aligned} \tag{E4}$$

By substituting (E4) in (E1) the EC at R can be written as

$$EC_R = -\frac{1}{\theta_r}\log_e(R_1\mathbb{E}_{z_{r2}}[e^{-C_{r,d_2}(k)\theta_r}] + R_2) \tag{E5}$$

APPENDIX F. CONDITIONS ON THE EC OF RELAY-D2D LINK

F.1 Condition I: ($\theta_d \geq \theta_r$)
We know that for a relay-D2D link operating under delay constraints at both transmitter and relay node, the overall EC is $EC_{D_2}^{D_1}(\theta_d, \theta_r) = \min\{EC_{D_1}, EC_R\}$. When the transmitter ($D_1$) operates under more strict delay constraints than the relay node (R) ($\theta_d \geq \theta_r$), EC_{D_1} acts as a limiting capacity because in this case $EC_{D_1} \leq EC_R$. Therefore, the overall link capacity will be

$$EC_{D_2}^{D_1}(\theta_d, \theta_r) = EC_{D_1}. \tag{F1}$$

The result in (F1) shows that under these circumstances, the EC of relay-D2D link is bounded by EC_{D_1}, and the presence of the buffer constraints at R does not affect the overall performance. We also observe that result in (F1) is only applicable when Z_{r_1} and Z_{r_2} have the same distributions and $\gamma_{d_1,r} \leq \gamma_{r,d_2}$. On the other hand, if $\gamma_{d_1,r} \geq \gamma_{r,d_2}$ then the overall EC of relay-D2D link will not be bounded by EC_{D_1} irrespective of the values of θ_d and θ_r. Therefore, in this scenario, bound on the overall EC of the link will be EC_R; thus, we can write

$$EC_{D_2}^{D_1}(\theta_d, \theta_r) = EC_R \tag{F2}$$

This shows that in the case of $\gamma_{d_1,r} \geq \gamma_{r,d_2}$, $R \to D_2$ link acts as a bottleneck irrespective of the QoS constraints imposed at D_1 and R.

F.2 Condition II: ($\theta_d < \theta_r$ and $\theta_r \leq \overline{\theta}$)

In this scenario, the relay node R is operating under more strict delay constraints than the transmitter, and constraints on R are also upper bounded by a unique QoS exponent $\overline{\theta}$, which provides the solution in (21). This unique QoS exponent $\overline{\theta}$ must always be greater and equal to θ_d. Therefore, in this condition, the overall EC of the relay-D2D link will be

$$EC_{D_2}^{D_1}(\theta_d, \theta_r) = EC_{D_1}. \tag{F3}$$

For $\overline{\theta}$, we must have the following equality satisfied (Appendix A[26])

$$EC_{D_1} = -\frac{1}{\theta_d}(\Lambda_{r,d_2}(-\theta) + \Lambda_{d_1,r}(\theta - \theta_d)) \tag{F4}$$

where $\Lambda_{r,d_2}(-\theta) = \log_e \mathrm{sp}(\boldsymbol{\Phi_2}(-\theta)\mathbf{R})$ and $\Lambda_{d_1,r}(\theta - \theta_d) = \log_e \mathrm{sp}(\boldsymbol{\Phi_1}(\theta - \theta_d)\mathbf{P})$. The log-MGFs are $\boldsymbol{\Phi_2}(-\theta) = \mathrm{diag}(\mathbb{E}_{z_{r_2}}[e^{-C_{r,d_2}(k)\theta}])$ and $\boldsymbol{\Phi_1}(\theta - \theta_d) = \mathrm{diag}(\mathbb{E}_{z_1}[e^{r_d(k)(\theta-\theta_d)}], 1, \mathbb{E}_{z_1}[e^{r_d(k)(\theta-\theta_d)}], \mathbb{E}_{z_{r_1}}[e^{r_r(k)(\theta-\theta_d)}])$.

F.3 Condition III: ($\theta_d < \theta_r$ and $\theta_r > \overline{\theta}$)

In case when delay constraints at R are lower bounded by a unique QoS exponent $\overline{\theta}$, there can be three scenarios.

$EC_R \geq EC_{D_1}(\theta_r)$

In case when the EC at R (EC_R) is greater or equal to the EC D_1 with θ_r as delay constraints at transmitter's queue ($EC_{D_1}(\theta_r)$)[¶] then the overall EC of relay-D2D link will be (Appendix A[26])

$$EC_{D_2}^{D_1}(\theta_d, \theta_r) = EC_{D_1}(\overline{\theta}^*) \tag{F5}$$

where $\overline{\theta}^*$ is the smallest solution to

$$EC_{D_1}(\overline{\theta}) = -\frac{1}{\theta}(\Lambda_{r,d_2}(-\theta_r) + \Lambda_{d_1,r}(\theta_r - \overline{\theta})) \tag{F6}$$

where $\Lambda_{r,d_2}(-\theta_r) = \log_e \mathrm{sp}(\boldsymbol{\Phi_2}(-\theta_r)\mathbf{R})$, $\Lambda_{d_1,r}(\theta_r - \overline{\theta}) = \log_e \mathrm{sp}(\boldsymbol{\Phi_1}(\theta_r - \overline{\theta})\mathbf{P})$, and $\boldsymbol{\Phi_1}(\theta_r - \overline{\theta}) = \mathrm{diag}(\mathbb{E}_{z_1}[e^{r_d(k)(\theta_r-\overline{\theta})}], 1, \mathbb{E}_{z_1}[e^{r_d(k)(\theta_r-\overline{\theta})}], \mathbb{E}_{z_{r1}}[e^{r_r(k)(\theta_r-\overline{\theta})}])$.

$EC_R < EC_{D_1}(\theta_r)$ **and** $EC_R \geq TB\log_2(1 + \gamma_{d_1,r}Z_{1,\min})$

In case when EC_R is upper bounded by $EC_{D_1}(\theta_r)$ and it must also satisfy the inequality $EC_R \geq TB\log_2(1 + \gamma_{d_1,r}Z_{1,\min})$ then the overall EC of relay-D2D link will be (Appendix A[26])

[¶]$EC_{D_1}(\theta_r) = -\frac{1}{\theta_r}\log_e \mathrm{sp}(\boldsymbol{\Phi_1}(\theta_r)\mathbf{P})$ where $\boldsymbol{\Phi_1}(\theta_r) = \mathrm{diag}(\mathbb{E}_{z_1}[e^{r_d(k)\theta_r}], 1, \mathbb{E}_{z_1}[e^{r_d(k)\theta_r}], \mathbb{E}_{z_{r1}}[e^{r_r(k)\theta_r}])$

$$EC_{D_2}^{D_1}(\theta_d, \theta_r) = EC_{D_1}(\bar{\theta}^*) \tag{F7}$$

where $Z_{1,\min}$ is the essential infimum of the Z_1, and $\bar{\theta}^*$ is the solution to $EC_{D_1}(\bar{\theta}) = EC_R$.

Otherwise

If none of the above conditions satisfies, then the overall EC of relay-D2D link will be

$$EC_{D_2}^{D_1}(\theta_d, \theta_r) = EC_R \tag{F8}$$